Master's thesis

NTNU
Norwegian University of Science and Technology
Faculty of Natural Sciences
Department of Biotechnology and Food Science

Celine E. Eidhammer

β-(1,3)-glucan-b-chitosan and β-(1,3)-glucan-b-biotin diblocks: Preparation, purification, and characterisation

Master's thesis in Industrial Chemistry and Biotechnology
Supervisor: Bjørn E. Christensen
July 2022

NTNU
Norwegian University of Science and Technology

Celine E. Eidhammer

β-(1,3)-glucan-b-chitosan and β-(1,3)-glucan-b-biotin diblocks: Preparation, purification, and characterisation

Master's thesis in Industrial Chemistry and Biotechnology
Supervisor: Bjørn E. Christensen
July 2022

Norwegian University of Science and Technology
Faculty of Natural Sciences
Department of Biotechnology and Food Science

NTNU
Norwegian University of
Science and Technology

Preface

This master's theis was conducted at the Department of Biotechnology and Food Science (IBT) at the Norwegian University of Science and Technology (NTNU) between January and June 2022. The SBG-b-biotin was prepared as a collaboration with the research group of Professor Dr. Christoph Rademacer of the University of Vienna's Molecular Drug Targeting (MDT) lab.

I would like to thank my supervisor Professor Bjørn E. Christensen for all the help and trust, and for giving me liberty in the research of diblock polysaccharides.

Thank to Senior Engineer Wenche I. Strand and Senior Engineer Olav A. Aarstad for the valuable help and guidance in the lab, and for conduction the HPAEC-PAD analysis on my behalf.

Also a special thanks to Amalie Solberg and Mina Gravdahl whom have always been there discussing all my many questions, and helping me along the way.

Most imporant thanks to my friends and family with all your unconditional love and support during these five years.

To all my closest friends, thank you for the many memorable moments at NTNU.
Day in, and day out.
Together we made it.

Trondheim, 01.06.2022

Celine E. Eidhammer

Abstract

The main goal of this master's thesis was to prepare SBG-b-chitosan and SBG-b-biotin diblocks, including the preparation and purification of SBG oligomers. Polysaccharides come from natural resources and are non-toxic, biocompatible and highly interesting in the field of medical applications. Due to their bioactivity and immunological interactions, preparing block polysaccharides from SBG, chitosan, and biotin was of great interest.

The objective of the first section of this thesis was to degrade low-molecular soluble β-(1,3)-glucans (SBG) by acid hydrolysis in order to obtain oligomers with a degree of polymerisation (DP), i.e chain length, between 1 and 25. A significant obstacle in the preparation of diblocks is the high concentration of salt resulting from degradation and the utilization of buffer solution. In this study, dialysis, a well-established purification technique, was compared to a recently introduced centrifugal filtration technique in an effort to potentially reduce purification time and increase the amount of mass preserved. However, the results demonstrated that the centrifugal filter failed to preserve the SBG oligomers and was therefore deemed ineffective for separating SBG from minor impurities.

In the second part of the thesis, SBG-b-chitosan diblocks were prepared, starting with terminal activation of SBG with the linker molecule O,O'-1,3-propanediylbishydroxylamine (PDHA). A comparison was made between the activation of a non-purified solution of hydrolysed SBG and a purified (dialysed) solution of hydrolysed SBG to determine if the high concentration of Na_2SO_4 in the hydrolysate affects reaction kinetics. Using time-course ^{1}H-NMR, the reaction rate between the two is concluded to be neglected, both resulting in a relatively high yield of ~ 85%. Thus, purification of SBG hydrolysate prior to preparation of SBG$_m$-PDHA is, based on this analysis is not necessary, reducing the number of steps in which product can be lost. Following, conjugation of SBG$_m$-b-chitosan was quickly obtained, with a yield of > 90% after only 30 minutes.

In the final part of this thesis, different SBG-b-biotin diblocks were prepared and compared to assess the transferability of the preparative protocol between SBG-

b-biotin diblocks of different chain lengths. The result showed that all tree chain lengths of SBG_m (4 < DP < 20) obtained approximately the same combined equilibrium yield of 60%. By increasing the molar equivalent from 2x to 4x between SBG_m and Biotin-PEG_3 the reaction rate increased, but the combined yield was unchanged. Therefore, additional research is necessary to optimize the preparative protocol in terms of conjugation yield.

Sammendrag

Målet med denne masteroppgaven var å forberede SBG-b-kitosan og SBG-b- biotin diblokker, inkludert fremstilling og rensing av SBG-oligomerer. Polysac- karider kommer fra naturlig rssurser og er ikke-giftige, biokompatible og svært interessante innenfor medisinske applikasjoner. På grunnlag av deres bioaktivitet og immunologiske interaksjoner, er preparering av blokkpolysakkarider av SBG, kitosan og biotin var av stor interesse.

Målet med den første delen av oppgaven var å bryte ned lavmolekylære løselige β-(1,3)-glukaner (SBG) gjennom syrehydrolyse, for å oppnå oligomerer med en grad av polymerisering (DP), dvs. kjedelengde, mellom 1 og 25. En betydelig hindring ved fremstilling av diblokker er den høye konsentrasjonen av salt som følge av nedbrytning og bruk av bufferløsning. I dette studie ble dialyse, en veletablert renseteknikk, sammenlignet med en nylig introdusert sentrifugerings teknikk med brukt av filter i et forsøk på å potensielt redusere rensetiden og øke mengden bevart masse. Resultatene viste imidlertid at filteret ikke klarte å bevare SBG-oligomerene og ble ansett som ineffektiv i separering av SBG oligomerer fra de mindre urenhetene.

I den andre delen av masteren ble det fremstilt SBG-b-chitosan diblokker og startet med terminal aktivering av SBG med linkermolekylet O,O'-1,3-propandiylbishydroksylamin (PDHA). En sammenligning ble gjort mellom aktiveringen av en ikke-renset løsning av hydrolysert SBG og en renset (dialysert) løsning av hydrolysert SBG, for å bestemme om den høye konsentrasjonen av Na_2SO_4 i hydrolysatet påvirker reaksjonskinetikken. Ved å bruke time course ^{1}H-NMR, konkluderes det med at reaksjonshastigheten mellom de to er neglisjerbar, hvor begge resul0tere i et relativt høyt utbytte på ~85%. Basert på denne analysen er dermed rensing av SBG-hydrolysat før fremstilling av SBG$_m$-PDHA ikke ansett som nødvendig, noe som reduserer antallet trinn hvor produktet kan gå tapt. Et høyt utbytte på konjugering av SBG$_m$-b-kitosan ble raskt oppnått, med en verdi på > 90% etter bare 30 minutter.

I den siste delen av ble forskjellige SBG-b-biotin-diblokker fremstilt og sammenlignet, for å vurdere overførbarheten av den preparative protokollen mellom SBG-b-biotin diblokker av ulik kjedelengde. Resultatet viste at alle de tre ulike kjede-

lengderne av SBG_m (4 < DP < 20) oppnådde omtrent samme likevektsutbytte på 60%. Ved å øke den molare ekvivalenten fra 2x til 4x mellom SBG_m og Biotin-PEG_3 økte reaksjonshastigheten, men utbyttet lå fortsatt på det samme. Derfor er ytterligere forskning nødvendig for å optimalisere den preparative protokollen når det gjelder konjugasjonsutbytte.

List of Abbreviations

221-7	batch of water-soluble β-1,3-glucan
AcOH	acetic acid
AmAc	ammonium acetate
A_nM	chitin, n-units of *N*-acetyl-D-glucosamine (A) with 2,5-anhydro-D-mannose reducing end (M)
A-unit	*N*-acetyl-D-glucosamine
b	linker molecule
BB	backbone
BCP	block copolymer
D_2O	deuterium oxide
DMSO	dimetyl sulfoxide
D_nM	chitosan, n-units of D-glucosamine with 2,5-anhydro-D-mannose reducing end (M)
DP_n	number average degree of polymerisation
DP	degree of polymerisation
FG	free glucose
^{1}H-NMR	proton nuclear magnetic resonance
HNO_2	nitrous acid
HPAEC-PAD	high-pH, anion-exchange chromatography with a pulse amerometric detector
HPLC	high-pressure liquid chromatography
LC	liquid chromatography
M_n	number average molecular weight
M-unit	2,5-anhydro-D-mannose
MQ	milli-Q
M_w	weight average molecular weight
MWCO	molecular weight cut-off

Na_2SO_4	sodium sulphate
NaAc	sodium acetate
NaCl	sodium chloride
NaOH	sodium hydroxide
PDHA	O,O'-1,3-propanediylbishydroxylamine
PB	α-picoline borane
PEG	polyethylene glycol
ppm	parts per million
rpm	revolutions Per Minute
RT	room temperature, 25 °C
SBG	water-soluble β-1,3-glucan
SEC	size-exclusion chromatography
TSP	3-(trimetylsilyl)-propionic-2,2,3,3-d4 acid
VLM-SBG	very low molecular soluble β-1,3-glucan

List of Figures

List of Tables

Contents

1 Introduction

1.1 Background

The possible applications of biopolymers are almost infinite and the interest in biodegradable polymers has increased as a result of their environmental benefits [9]. In an attempt to draw attention away from synthetic polymers, frequently derived from petroleum and non-renewable resources, new techniques for the use of polysaccharides as copolymers are developed, optimizing their properties and diversity. Their biocompatibility, non-toxicity and wide availability allow for a variety of uses in the fields of biomaterials, disinfectants, and pharmaceuticals [3]. Most importantly, their use in medical applications has expanded in the use in wound closure and healing products, surgical implant devices, and drug delivery systems [9].

Block polysaccharides consist of two or more polysaccharides that have been chemically engineered to retain the inherent intrinsic properties. Through terminal linkage of the reducing end, the physicochemical properties of the block polysaccharides have been shown to resemble those of synthetic block copolymers. Using click chemistry, various block polysaccharides, including alginate-b-dextran [10], chitosan-b-dextran [2], β-glucan-b-dextran [11], etc., have been successfully synthesised. The preparational protocol for such diblock are somewhat similar, and transferable into other diblocks with only minor modifications. This enables a variety of different diblocks, all depending on the polysaccharide combination. Consequently, diblock polysaccharides are of high interest containing multiple possibilities in the field of green chemistry. [12]

Regarding medical applications of block polysaccharides, β-glucans and chitosan are particularly interesting due to their bioactivity and immunological interactions [13;14]. β-glucans with multiple biochemical reactions and/or interactions involving stimulation of viral responses [15], antitumor activity, and interactions with immune cells [16]. According to Biotech Pharmacon ASA, SBG has an effect in cancer, wound care-diabetic ulcer and inflammatory bowel disease (IBD) [17]. And chitosan, with its nucleic acid interaction property enabling formation of binary polyelectrolyte complexes [18].

1.2 Aim

The aim of my master's thesis was to prepare SBG_m-b-D_nM and SBG_m-b-Biotin diblocks. In order to do so, SBG oligomers had to be prepared and purified prior to preparation of both diblocks. The project is therefore divided in three main sections corresponding:

1. Preparation and purification of SBG_m oligomers.
2. Develop a preparative protocol for SBG_m-PDHA-D_nM diblocks.
3. Optimise the preparative protocol and obtain kinetics data for SBG_m-PEG_3-Biotin diblocks.

A preparative protocol for SBG oligomers has previously been established[3] and was chosen to achieve oligomers of low molecular weight (DP ~ 5-20). During this degradation, a solution difference in the SBG batch 221-7 and VLM-SBG was observed. A solution study was therefore of interest to possibly discover the reasons for this differences, and if/how this could effect the research. Following, to optimize the purification step in regards to the time and mass preservation, different desalting methods were analysed.

Prior to preparation of SBG_m-PDHA-D_nM diblocks, a protocol for direct activation of polydisperse SBG hydrolysate was developed. This was inspired by an established protocol for PDHA activation of a beforehand separated SBG_m oligomer solution DP[3;11]. Additionally, activation of non-purified SBG hydrolysate with purified (desalted) was compared. All with an aim of shortening down the preparative protocol and reduce loss of mass during purification.

The preparation of SBG_m-PEG_3-Biotin diblocks was conducted as a request from Professor Dr. Christoph Rademacer, at the Molecular Drug Targeting (MDT) lab, University of Vienna, in their research on cell response analysis of SBG_m-b-Biotin diblocks. In my related specialisation project during fall of 2021, a preparative protocol for SBG_m-PEG_3-Biotin was developed. An optimisation of this protocol was therefore conducted, as well as analysing the reproducibility and use of this protocol with different chain lengths of SBG.

2 Theory

2.1 Block copolymers

Block copolymers (BCPs) are composed of two or more chemically distinct monomers covalently bond together forming blocks, enabling the creation of novel structures and materials. The blocks vary in origin and length, have a high degree of complexity, and possess a wide range of chemical and/or physical properties. Structurally, the copolymers can be configured into linear block copolymers, "Comb" graft copolymers, star copolymers, etc. These compositional and structural diversities are the motivation for an expanding research that leads to innovative synthetic strategies [19].

Polysaccharide-containing blocks and polysaccharide blocks are copolymers that partly or exclusively contains polysaccharides, being a more sustainable alternative to pure synthetic copolymers [20]. They are mostly synthesised through direct end-to-end coupling of two or more polysaccharides via a linker molecule producing AB diblock, ABA/ABC triblocks, etc., as shown in figure 1. The linker molecules symmetrical structure enables click conjugation with the reducing ends of the polysaccharide, resulting in antiparallel chains [12]. Examples of linker molecules are O,O'-1,3-propanedidylbishydroxylamine (PDHA) and polyethylene glycol (PEG), described more in detailed in Section 2.5 [3;21].

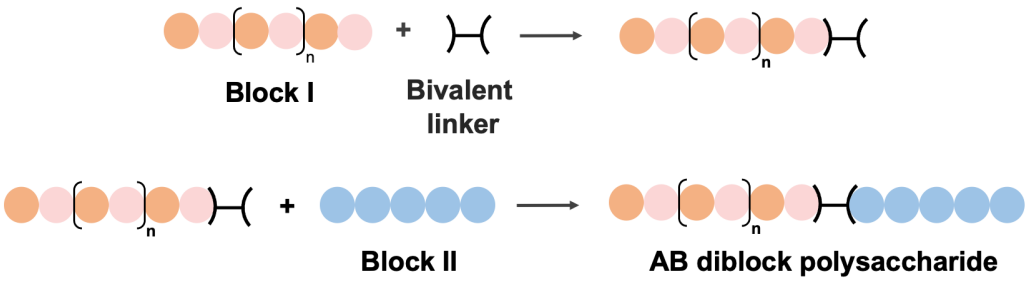

Figure 1: Illustration of end-to-end AB diblock polysaccharide preparation through activation of the reducing ends of block I and subsequently block II, with a bivalent linker molecule.

A property of high interest in the field of medicine, is block copolymers self-assembly, as illustrated in Figure 2. It has received increased attention in the manufacture of nanoparticles [22]. The micelles usually consist of a hydrophobic core and hydrophilic shell and are suitable carries for drugs with low water solubility and/or low water stability. The binding of polysaccharides with different intrinsic properties in creation of such micelles enables many possibilities in drug delivery systems, such as vaccine technology [23].

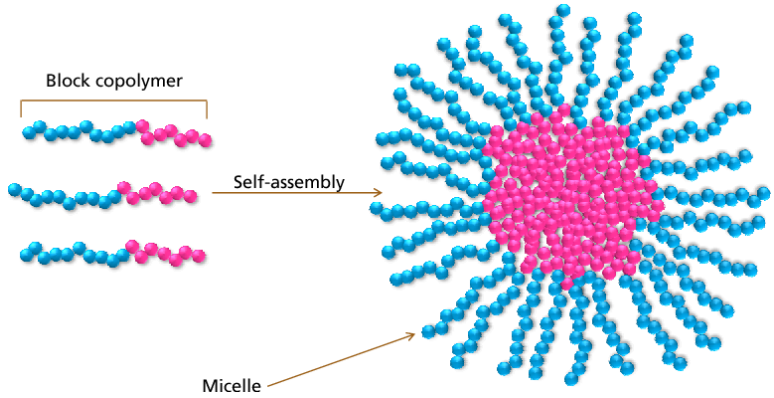

Figure 2: Illustration of copolymers and their self-assembly forming a micelle. [1]

2.1.1 Reducing ends in sugars

Polysaccharides are polymers containing multiple monosaccharide units covalently linked together through a glycosidic linkage [24]. They can consist of reactive or non-reactive functional groups, or being unfunctionalized with a large number of secondary and/or primary hydroxyl groups. These hydroxyl groups have relatively low reactivity due to structural limitations. However, the reactivity of end-sugar of the polysaccharide chain differ from the rest, being significantly higher. This end is called reducing end and implies to the anomeric carbon that is not involved in a glycosidic bond.

As shown in Figure 3, the reducing end is in a equilibrium between an open and a closed ring structure, more dominantly as a closed ring structure. The increased reactivity is due to the free electrophilic aldehyde group which can produce new functional groups for chain extension, coupling, and so on. Reductive amination and oxime ligation are examples of reactions utilizing the reactivity of the these

reducing ends [20].

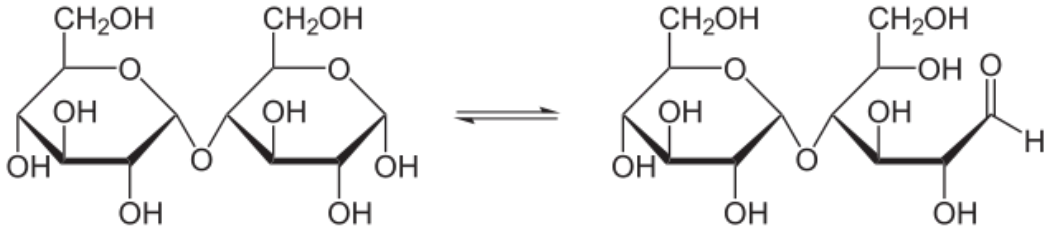

Figure 3: Equilibrium between open and closed structure of reducing ends sugars. In terminal conjugation, the aldehyde in the open ring structure is the reactive component.

2.2 Soluble β-glucans (SBG)

β-(1,3)-glucans are high-molecular polymers made of repeating units of D-glucose residues linked through β-(1,3) linkages. They are a natural part of the cell wall of many different organisms including bacteria, fungi, and plants, serving as a skeletal or structural component. Some exist as complete linear and unbranched polysaccharides, whilst others consist of some branching units with β-(1,6) linkages, as shown in Figure 4. The frequency of such branches is determined by the origin of the β-glucans and the polymer's physicochemical properties [24;25]. For instance, the cell wall dry weight of a Baker's yeast, *Saccharomyces cerevisiae*, may consist of up to 30% β-(1,3)-glucans [26]. Extraction method is also effecting the physical and chemical composition [27;28].

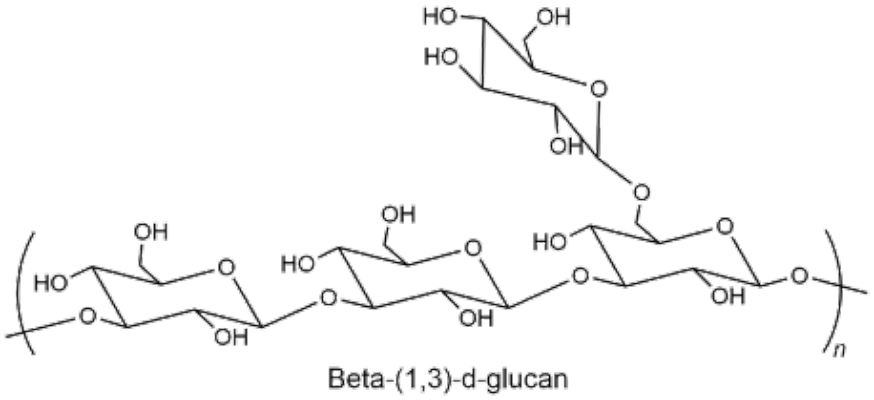

Figure 4: Chemical structure of β-1,3-glucan with β-1,6 linked side chains- Note that the number of monomers at the side chain can vary and does not always occur as a single monomer as depicted in this structure.

2.2.1 Chemical and soluble properties

Previous research [29] has indicated that soluble β-(1,3)-glucans (SBG) consists of an average of 5 branching points each 100 residues in the β-(1,3)-glucan backbone [29]. However, the precise chemical composition of SBG has not been reported [17]. The solution properties of SBG are dependent on the molecular size and chemistry [25], resulting in a variety of physiochemical properties of SBG despite having structures that are essentially identical [30]. In general, long, linear, and unbranched SBG chains are less soluble in water than shorter chains with more branching points [31]. An alternative solvent is DMSO, which has proven to dissolve SBG at high chain lengths [32].

2.2.2 Degradation through acid hydrolysis

Degradation of SBG oligomers using acids such as hydrochloric acid (HCl), sulphuric acid (H_2SO_4), phosphoric acid (H_3PO_4), or nitric acid (HNO_3) is quick and effective. Unlike enzymatic/physical degradation, it does not require pre-treatment to break down the glycosidic bond. Acid hydrolysis is usually conducted with a concentration of 1 $\sim$ 10 % HCl or H_2SO_4, at 100 $\sim$ 150 °C [33]. Valuable purification methods following the hydrolysis is necessary because the use of acid and neutralisation leads to high amount of salt in the solution [34].

2.2.3 Bioactivity and medical applications

One of the reasons why SBG is of such interest in biopolymer chemistry, except coming renewable sources, is its non-toxicity, biodegradability, and bioactivity. Overall, SBG interacts with multiple biochemical and immunological reactions, stimulating responses against viral [15], and fungal infections [35]. Long has it been known that fungal β-(1,3)-glucans can protect against lethal viral infections in studies with mice [36]. Additionally, SBG have been reported to activate the alternative complement pathway [29], stimulate macrophages phagocytosis [?], and antitumor activity producing cytokines, including TNF-α [37;16]. Thus, it increase the non-specific disease resistance [38]. Altogether making them highly interesting in the field of medical devices and drug delivery [17].

2.3 Chitin and chitosan

Chitin is a naturally abundant polysaccharide with more than 1000 tons produced each year [39]. It is the main component in the exoskeleton of crustaceans and insects, as well as the cell walls of yeast and fungi. Thus, large quantities of chitin are available as a by-product of the aquaculture [39;6]. Chitosan is naturally less available, but can be isolated from the mycelia of the fungus *Mucor rouxii* [3]. It is, alike chitin, a nontoxic, biodegradable and bioactive polymer of high interest in the field of biomedical engineering [39]. Mixing polyanionic molecules such as nucleic acids with chitosan, a catiotic biopolymer, binary polyelectrolyte complexes are spontaneously are formed [18]. A property of great interest to future RNA-based technology research.

Both chitin and chitosan (Figure 5) consist of β-1,4-linked N-acetyl-D-glucosamine (A, GlcNAc) residues and de-acetylated D-glucosamine (D, GlcN) residues [39]. The difference in structre between the two is the fraction of GlcNAc residues (F_A) were commercial chitosan typically have a F_A between 0.10 and 0.20 [24]. Thus, chitosan having positive charges groups have a pK_a = ~ 6.5, meaning it is neutral at a pH > 6.5 [24]. The positively charged amino-groups makes it soluble in water at low pH.

Terminal conjugation of chitosan (D-reducing end) has proven to have low reactivity. Because of that, 2,5-anhydro-D-mannose (M-unit) has been introduced as reducing ends creating D_nM oligomers with much higher reaction kinetics [3]. The M-unit is developed during nitrous acid depolymerization of chitosan, a mechanism that deaminates the D-unit forming the M-reducing end of the cleaved oligomer [40].

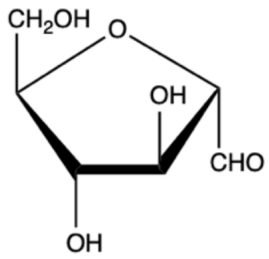

Figure 5: chemical structure of chitosan with a 2,5-anhydro-D-mannose (M-unit) reducing end [2]

2.4 Biotin-PEG$_3$ oxyamine

Biotin is a water-soluble vitamin and coenzyme of the essential methabolic carboxylases, a multicomponent enzyme [41;42]. The enzyme s extensively dispersed in nature and play crucial roles in fatty acid metabolism, carbohydrate metabolism, amino acid metabolism, urea utilization, and other cellular processes. [43;44] Additional, biotin's involvement in epigenetic regulation of genes, chromatin structure, and cell signaling has opened up a vast array of potential medical applications [41]. One of particular interest is biotin's ability to bind antibodies, antigens and enzymes through avidin-biotin interactions [45]. Hence, it is associated with immunological processes, therefore biotin can serve as a marker for drug administration, lymphocyte activation, and immunoassays. [46]

Biotin-PEG$_3$ oxyamine, illustrated in figure 6, consists of the biotin subunit that is stably bound to PEG through a flexible amino linkage (secondary amines). The reactive oxyamine facilities direct click chemistry with the desired polysaccharide, creating block polysaccharides with PEG$_3$ as linker molecules [3]. This block polysaccharides can be used in direct drug delivery with biotin as an surface receptor. Even though PEG is approved as a synthetic polymeric therapeutic, using a such linker molecule does not result in an entirely non-synthetic block polysaccharide [47].

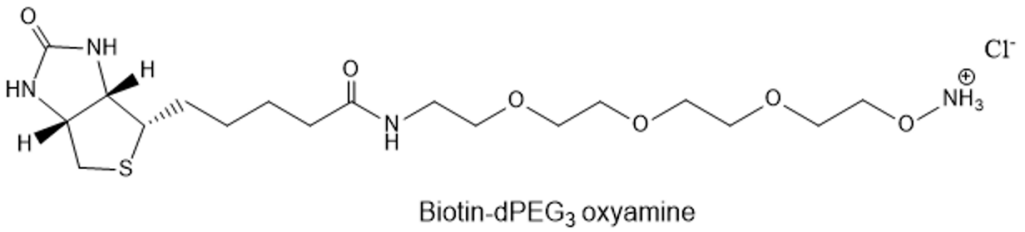

Figure 6: Chemical structure of biotin-dPEG$_3$ oxyamine.

2.5 PDHA and PEG as linker molecules

O,O'-1,3-propanedidylbishydroxylamine (PDHA), and poly(ethylene glycol) (PEG) oxyamine are both polymers with a carbon backbone, as displayed in Figure 7a and Figure 7b, respectively. The symmetrical structure of PDHA consisting of reactive oxyamines at both ends makes it attractive as linker molecules in block chemistry[4]. Similarly, oxyamine reactive ends can exist in PEG, resulting in the same reaction mechanism. The conjugation between oxyamines and the reducing ends of the polysaccharides is reversible, creating acyclic oximes ((E)- and (Z)-confirmation) and cyclic N-glucosides, all in equilibrium. The stability of these structures varies considerably, and the use of a reducing agent such as α-picoline borane would strengthen their stability[4;48]. Note that a conjugation between an M-unit reducing ends, only acyclic oximes are formed[6].

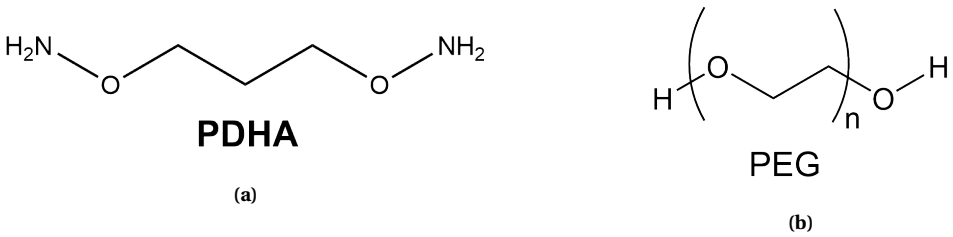

Figure 7: The chemical structures of **a)** O,O'-1,3-propanedidylbishydroxylamine (PDHA) and **b)** poly(ethylene glycol) (PEG) oxyamine.

2.6 Reductive amination - click chemistry

Block polysaccharides are terminally conjugated through reductive amination, a widely used "click" reaction for terminally and laterally modification of polysaccharides. It is a two steps condensation reaction (Figure 8 between a carbonyl group (usually reducing end) and an amine derivative (linker molecule) forming a Schiff base (e.g. (E)-/(Z)-oximes). Following, the formed linkage is ireveribly reduced to stable secondary amine using a reducing agent such as α-picoline borane (PB), sodium cyanoborohydride ($NaCNBH_3$), etc.[49;10;50].

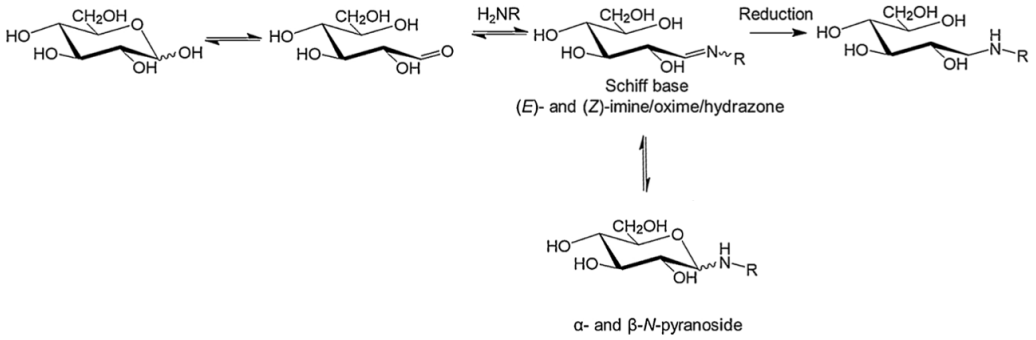

Figure 8: Chemical reaction of reductive amination involving a carboxyl group and an amine [3]

In polysaccharides, the reducing end residue is in equilibrium with an aldehyde and a cyclic hemiacetal structure having α and β reducing ends. The reaction kinetics is dependent on temperature, pK_a of amine derivative, and pH since protonation of the carbonyl group is dependent on the pH. The reaction rate increases with decreased pH as the carbonyl group is sensitive to. Optimal reaction conditions for the carbonyl group and the amine derivative is therefore above the pK_a of the amine derivate, but at a low pH reaction [51]. I.V Mo *et al.* has reported successful conjugation using a buffer solution of 500mM NaAc at pH 4 [4].

2.6.1 α-picoline borane (PB) as reducing agents

The secondary step in the reductive amination of polysaccharides requires the presence of a reducing agent, in an irreversible reaction creating stable secondary amine (Figure **??**). A commonly used reductive agent is sodium cyanoborohydride ($NaCNBH_3$). It favors aldehydes and ketones at a low pH (3-4) and imines at higher pH (6-8). This selectivity of reduction leads to limitations in reduction of conjugated polysaccharides, as the reducing agent is added to the conjugate solution, usually having pH $\sim$ 4. Additionally, $NaCNBH_3$ is highly toxic and produces toxic byproducts that may contaminate the product [49;50], an unwanted situation if the block polysaccharides are to be used in medical applications.

α-picoline borane (PB)(Figure 9) has been introduced to the reductive aminations as it is non-toxic, cheap, commercially available, and equal, or more, efficient [52]. Sato *et al.* introduced it as a greener alternative that has proven high efficiency in water, a big advantage working with reactions of water-soluble polysaccharides [53].

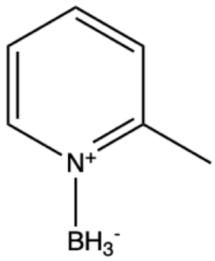

Figure 9: Chemical structure of α-picoline borane (PB) [4]

2.7 Analytical methods and techniques

2.7.1 Chromatography

Chromatography is a well-known technique that enables the separation, identification, and purification of a mixture of different components. The components' size, shape, total charge, and interaction with a stationary phase are characteristics that are used to separate and thus purify a specific substance in a mixed solution. Chromatography is thereby an important technique in biochemistry, protein purification, among others. Currently, a variety of chromatography methods exists including thin-layer chromatography (TLC), gas chromatography, high-pressure liquid chromatography (HPLC) and column chromatography as the most acclaimed one. [54]

There are various types of separation techniques that use different characteristics and interactions, such as ion exchange, partition, surface adsorption, and size exclusion, where the latter separate the substances based on their size. The common denominator for all of these techniques is that it contains a stationary phase and a moving mobile phase. The stationary phase is usually a solid phase or a liquid solution coated on the surface of a solid. The mobile phase on the other hand is either a liquid, then called liquid chromatography (LC) or gas, referred to as gas chromatography (GC).

The desired components are located in the mobile phase and due to different interaction with the mobile phase, their time in the chromatography system varies. If a substance has a high affinity, adsorption or partition towards the stationary phase it will move more slowly throughout the system then substances with low affinity, adsorption or partition. The amount of time the substances use in the system will thereby variate, thus a separation can be achieved. Components with approximately the same particular characteristic is therefore difficult, if not impossible, to fully separate. In such cases, other chromatography methods using another characteristics of the components may be considered. [54]

Size-exclusive chromatography (SEC)

Size-exclusion chromatography (SEC) is a well-known column chromatography that used the difference in hydrodynamic volume, i.e. size and shape, of the components in a mixed solution. Hence, SEC is highly suitable for biopolymer solutions as they are mostly dispersed with a wide molecular weight distribution [55]. The columns in the SEC system consist of porous particles as the stationary phase. Smaller molecules will penetrate into the pores, delaying the movement through the column. Larger molecules on the other hand will not penetrate and therefore move faster through the column [56;55;57]. The separation is illustrated in Figure 10.

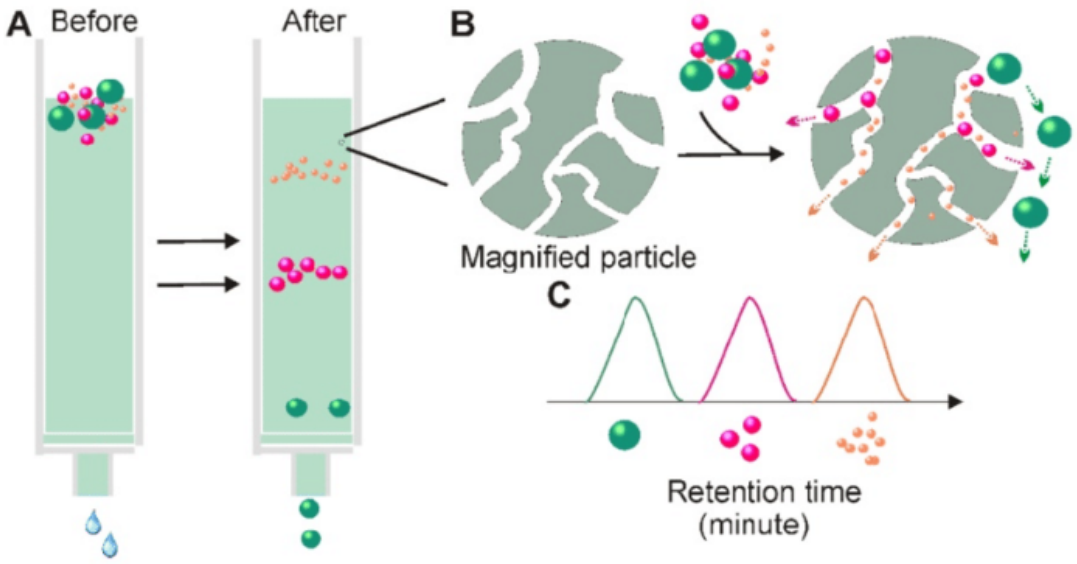

Figure 10: A schematic representation of size-exclusive chromatography and the separation of different sized molecules [5]. **A** The column and the flow of molecules in the column. **B** Magnified picture of the particles and how small molecules are delayed by these particles. **C** Chromatography with differed retention time depending on size.

HPAEC-PAD analysis

High-pH, anion-exchange chromatography (HPAEC) is a liquid chromatography with a higher sensitivity than compared to size-exclusive chromatography. The stationary phase of the columns contains more or less permanently bound charged groups, which enables ion-ion interaction. The mobile phase consist of a buffer solution with known pH and ionic strength.

The polysaccharide, which is dissolved in the mobile phase, is pumped through the column under conditions that promote reversible interactions. Since polysaccharides are polyhydric compounds and considered weak acids, negatively charged oxyanions are formed when dissolved in basic solutions. These oxyanions may interact with the anion-exchange columns and delaying the elution time. When a polydisperse solution of a specific biopolymer is injected in the column, the larger polymers will elute later than smaller ones as they contain more charged groups. Hence, the molecular size increases with increased elution volume. The separation is analysed through a pulse amerometric detector (PAD) transforming the data into a readable chromatogram [56].

2.7.2 ^{1}H-NMR spectroscopy

Nuclear Magnetic Resonance (NMR) spectroscopy is the single-most important analytical instrument for characterizing organic substances in the field of biochemistry and biopolymer chemistry. [58]. Based on a strong magnetic field and the quantum mechanical properties of a nucleic atom, different characteristic behaviors of a nuclei can be detected [24]. The different nuclei behaviors provide data of the structure and the presence of functional groups within an organic compound [58].

In proton NMR (^{1}H-NMR), the atom of interest is hydrogen having a proton as nuclei. This proton carry a charge with a magnetic dipole. Under the influence of an external magnetic field, the proton of the hydrogen atoms absorbs and re-emits detectable electromagnetic radiation. This concept is based on a so called *nuclear spin*, or just "spin", and describes the intrinsic angular momentum associated with the magnetic field. With no external force, the magnetic moment of the nuclei is pointed in the direction of the dipole's magnetic field. However, during external force the momentum will align with or against this external magnetic field [58]. For hydrogen ($^1_1$H), the spin number I is $\frac{1}{2}$. Other nuclei have different spin numbers depending on atom mass and atomic number [58].

For a nuclei with spin number $\frac{1}{2}$ such as hydrogen, the number of energy levels is two which are designated as α and β. The energy difference between the two states are given by

$$\Delta E = h\nu \tag{1}$$

where h is a constant and ν is the applied radiofrequency. The radiofrequency applied by the instrument is usually given in megahertz (MHz) and can for instance be 300 mHz NMR spectrometer or 600 mHz NMR spectrometer. When the sample is placed in the magnetic field, a small pulse of high-power radiofrequency is applied. In ^{1}H-NMR, the hydrogen nuclei in the lower energy state (α) excites to a higher the higher energy level (β). When the nuclei flip back to the lower state, energy is released, creating a detectable signals [58]. These signals are recorded and converted to a readable spectra as shown in Figure 11.

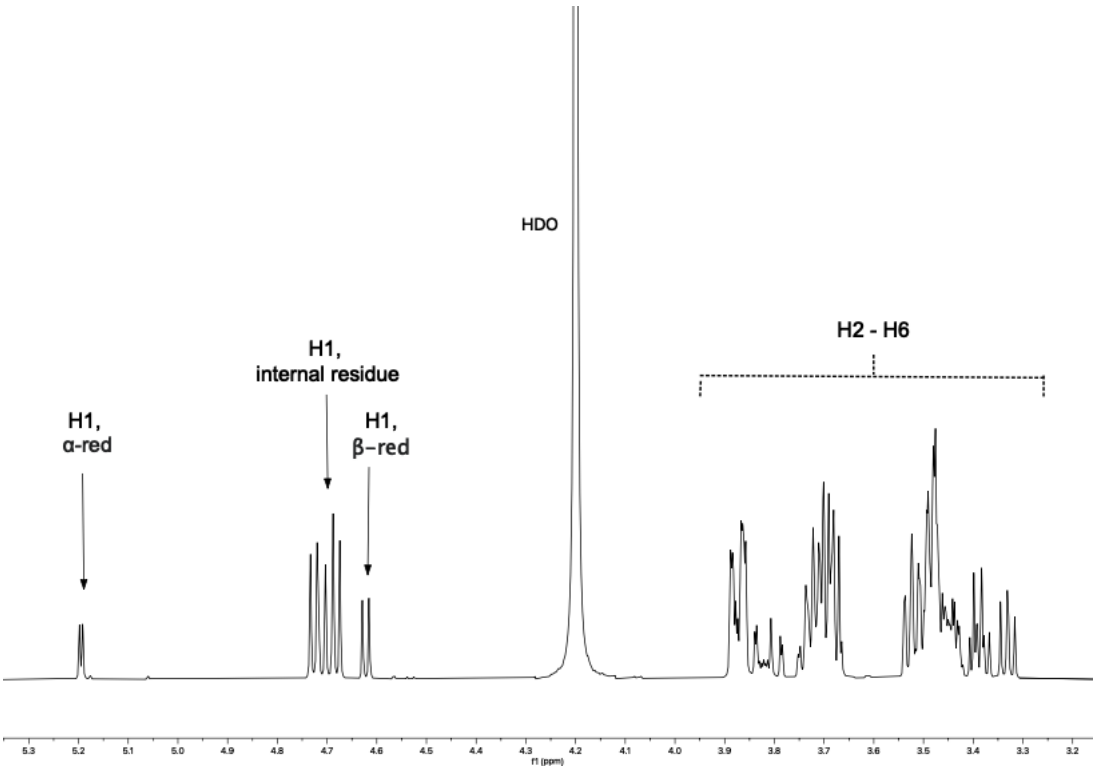

Figure 11: ^{1}H-NMR spectra of SBG oligomer (Laminaritetraose, DP = 4) at 82°C, 600MHz.

An organic compound consists of many atoms closely located around each other. The electron in these atoms affects the experienced magnetic field of a proton, creating a phenomenon called shielding. The shielding occurs to a very small extent (parts per million (10^{-6}, ppm), and depends on the chemical environment around

the hydrogen. In other words, multiple neighboring electrons leads to more shielding and lower frequencies. This enables a variation in reference frequencies referred to as chemical shifts. A high chemical shift (in ppm) corresponds to more shielding, and vise versa. Through analysing the integral under the chemical shifts, the relationship between the peaks can be determined. Subsequently, determining the number of protons in a specific environment. This relationship, given in Equation 2, is fundamental in determining the chain length of polysaccharides, as the number of protons in the reducing end can be compared to the number of protons in the internal residues [58].

$$DP = \frac{H1_{Internal} + H1_{red-end}}{H1_{red-end}} \tag{2}$$

2.7.3 Dialysis

Dialysis is a procedure in which larger molecules can be separated from minor molecules through membrane technology. In biopolymer chemistry this usually applies to separating the biopolymer from salt and other smaller impurities, using the technique as a purification method. The way it works is that the polymer solution is added into a dialysis bag that contains a certain pore size. It is then dialysed against either pure water, salt water or pH adjusted water. During this process, small molecules diffuses through the membrane until an equilibrium between the outside and inside of the bag is achieved. This results in a lower concentration of the impurities inside the dialysis bag [2;24]. This is driven by a difference in osmotic pressure, creating a concentration gradient between the inside and outside. A grater concentration gradient results in a higher decrease of impurities in the bag [59]. Which molecules that are retained inside the bag, is defined by the molecular weight cut-off (MWCO). This value replies to the minimum molecular weight of a spherical molecule that is remained in the bag. Since the shape of the polymers varies depending on the type, some polymers still retain in the dialysis bag even with a lower molecular weight [2;24].

3 Materials and methods

3.1 Materials

Water-soluble VLM-SBG (SBG, M_w = 35 kDa, Mn = 9.1 kDa, DPn = 56) and 221-7 SBG war both isolated from the cell wall of *saccharomyces cerevisiae* and provided as freeze-dried material by Biotec BetaGlucans AS (Tromsø, Norway). In-house SBG_{14} and SBG_{15-19} prepared by I.V Mo and A.Solberg (2019/2020), and SBG_4 (laminaritetraose) obtained from Megazyme were used in the SBG-b-biotin diblocks. In-house chitosan prepared by J. E. Pedersen (2020). containing a 2,5-anhydro-D-mannose (M-unit) reducing end, was used in the SBG-b-chitosan diblock. O,O'-1,3-propanediylbishydroxylamine (98%) (PDHA), α-picoline borane (Pic-BH3/PB), deuterium oxide (D_2O), acetic acid-d4 ($AcOH_{d4}$), and 3-(trimetylsilyl)-propionic-2,2,3,3-d4 acid (TSP), were purchased from Sigma-Aldrich.

3.2 Size-Exclusive chromatogram (SEC)

The use of size-exclusive chromatography included separation and purification of samples. A system containing three Superdex 30 columns (HiLoadTM 26/600 (26 mm and 600 mm) with a sodium chloride (NaCl) buffer (0.1 M, pH 6.8) with 0.8 ml/min flow rate was used. The solution is eluded through the columns by a LC-10AD vp SHIMADUZY pump. Separation was monitored by a RI detector (SHODEX RI - 101) detector and collected by a fractionator (System 1: Frac-100, Pharmacia Fine Chemicals).

3.3 HPAEC-PAD

Preparative protocol was provided by Senior Engineer Olav A. Aarstad.
High-performance anion-exchange chromatography (HPEAEC) with pulsed electrochemical detection (PAD) on a Dionex ICS 5000+ system (Thermo Scientific) with a 4x250 mm CarboPac PA100 main column and a 4x50 mm guard column. For β-glucans, samples were eluted at 24°C with isocratic 0.1 M NaOH and a linear sodium acetate (NaAc) gradient of 10 - 610 mM in 90 minutes. After the method, a 15 minute equilibration step with 0.1M NaOH and 10 mM NaAc was included.

Samples were dissolved in MQ water to a concentration of 0.2 - 1 mg/ml before injection (25 µl). A mixture of β-(1-3)-oligomers (laminaran) with DP 2-6 was used as standards and Waveform A (Gold-Ag-AgCl Re, Carbo, quad) was used for detection. Data were collected and processed with Chromeleon (Thermo Scientific) 7.2 software.

3.4 Proton nuclear magnetic resonance (^{1}H-NMR)

Samples were dissolved in D_2O (475-600μl) or deuterated NaAc buffer (500mM, pH 4, 2 mM TSP) and transferred to 5 mm NMR tubes. 1D ^{1}H-NMR analysis was conducted at 25°C or 82 °C, using a Bruker NEO 600 MHx spectrometer. The NMR spectra was analysed in MestReNova v14.2.1-27684.

3.5 SBG oligomer preparation and characterisation

3.5.1 Acid hydrolysis of SBG

SBG (Batch 221-7, VLM-SBG) was dissolved in MQ water during continuous stirring (200 rpm) overnight. Pre-heated SBG (5 mg/ml, 99°C) was hydrolysed with pre-heated H_2SO_2 (0.1M, 99°C) for 75 min at 99°C, then cooled and neutralised with NaOH until pH 7 was obtained. The solution was dialysed (MWCO = 3.5kDa) against MQ to a conductivity in bucked < 2μS/cm.

3.5.2 Solubility of batch 221-7 and VLM-SBG

Hydrolysed and starting bathc of SBG (221-7) (10mg) and VLM-SBG (10 mg) was dissolved in MQ at RT and 99°C (5 ml), and DMSO (5 mL) to evaluate its solubility.

3.6 Desalting methods for SBG oligomers

3.6.1 Desalting with dialysis

Hydrolysed SBG containing N_2SO_4 was dissolved overnight in MQ (7.0 mg, 17,6 mL), with continuous stirring. The concentration of Na_2SO_4 was determined by comparing the conductivity in the dialysis bag at different times (~ 3 days á 3 measurements), with a prepared standard curve of Na_2SO_4. Following, the weight per-

cent of Na_2SO_4 in the SBG_m hydrolysate was calculated. The standard curve and its preparation is given in Appendix C

3.6.2 Desalting with Centricon filtration

SBG hydrolysate (221-7) containing approximately 70 wt% Na_2SO_4 filtrated 70 ml at a time. Centricon Plus-70 membrane was filled with 70 mL MQ and spinned (3500 rcf) for 5 minutes to trace amounts of glucerine. 70 ml sample is filled in 4 different Centricon membranes and spinned for 60 minutes. The resulting sample was decanted, refilling the filter with 70ml solution as many times as necessary. After use, 10 ml MQ i spinned for 3 min so that the filter is not stored when dry.

3.7 Preparation and characterization of polydisperse SBG_m-PDHA

3.7.1 Terminal conjugation of SBG_m=PDHA, using time-course ^{1}H-NMR

Hydrolysed VLM-SBG/Batch 221-7 SBG (10-20mM, DPn ≃ 8) was conjugated with 10x PDHA (100-200mM) in NaAc/deuterated NaAc buffer (500mM, pH 4.0)/(500mM, pH 4.0, 2mM TSP) for 48h at RT and reduced with 20x PB (200-400mM) for 48h at 40°C. Prior to reduction, a sample (100 µg) was collected and characterized by NMR as described in Section 3.4 to confirm activation. The reduction was terminated by dialysis (MWCO = 3,5kDa) against salt (0.05M NaCl) until no precipitation of PB was observed, and against MQ until conductivity in bucket < 2µS/cm. It was freeze dried and the reduced SBG_m-PDHA was validated with NMR.

3.8 SBG_{10}-PDHA-MD_{11} diblock

SBG_{10}-PDHA and 1x equivalent (M-unit) in-house DnM was dissolved in deuterated NaAc buffer (deuterated NaAc buffer, pH 4.0, 2 mM TSP) over night while being stirred using a rotary mixer. The solvents was mixed in a NMR tube, and conjugated at RT for 24h while being studied by time-course NMR at RT for 24h. Following, the conjugates was reduced with 20x PB at 40°C for 72h, and dialysed against salt (0.05M NaCl x2) and MQ until the conductivity in bucket < 2µS/cm. The diblock was freeze-dried and characterized with ^{1}H-NMR.

3.9 SBG_n-PEG_3-Biotin diblocks

3.9.1 Preparation of SBG_n-PEG_3-Biotin diblocks

In house SBG (DP = 4, 14 & 15-19) and Biotin-$dPEG_d$ oxyamine (Sigma-Aldrich..) was dissolved separately in NaAc buffer (500 mM, pH 4.0, RT, 2mM TSP) overnight using a rotary mixer. SBG (10 mM) was was conjugated with 2x Biotin-PEG3 (20 mM) for 48h at RT (22°C) and reduced with 20x PB (200 mM) for 125h (5 days) 40°C. The reduction was terminated by dialysis (MWCO = 3.5 kDa) against salt (0.05M NaCl, x2) and MQ until conductivity < 2µS/cm and freeze dried. The conjugated SBGn-PEG3-Biotin was purified by SEC, freeze dried and characterized by ^{1}H-NMR.

4 Results

The objective of this master's thesis was to prepare and compare SBG oligomers from batch 221-7 and VLM-SBG. Following this, SBG-b-chitosan and SBG-b-biotin diblocks were prepared and characterized. Thus, the results are given in three main parts. Part one includes preparation and purification of SBG, given in Section 4.1 and Section 4.2, respectively.

Secondly, SBG-b-chitosan diblocks were prepared, starting with terminal conjugation and reduction of SBG with PDHA linker molecule, presented in Section 4.3. Section 4.4 presents the result from time-course analysis of the SBG-b=chitosan preparation.

The third part consist of SBG-b-biotin diblocks. Three different chain lengths of the diblock was prepared; SBG_4-b-biotin, SBG_{14}-b-biotin and $SBG_{(15-19}$-b-biotin. Additionally, SBG_4-b-biotin was prepared with two different reaction proprieties. Time-course conjugation of the SBG-b-biotin diblocks is given in Section 4.5.1. Section 4.5.2 and Section 4.5.3 includes amine reduction of the diblocks, and purification and characterization. The SBG-b-biotin was prepared in collaboration with Professor Dr. Christoph Rademacer of the University of Vienna's Molecular Drug Targeting (MDT) lab. Their objective is to investigate the cellular response of SBG-b-biotin diblocks for possible medical applications.

4.1 SBG oligomer preparation and characterisation

In the process of preparing SBG-based diblocks, SBG oligomers had to be isolated and characterized. This started with degradation of low molecular SBG (221-7/VLM) though acid degradation, presented in section 4.1.1. Towards degradation, a difference in solubility of batch 221-7 and VLM-SBG was observed, both before and after degradation. Therefore, in an attempt to discover possible reasons for the differences, a solvent analysis was conducted to observe precipitation or clear sample with different solvents.

4.1.1 Acid hydrolysis of SBG

Previous analysis of degradation of SBG oligomers from batch VLM-SBG has resulted in a disperse distribution of SBG oligomers using method described in section 3.5.1 [3]. As a preparative step for isolating SBG oligomers, samples from both batch 221-7 and VLM-SBG were degraded. To validate the distribution of degraded SBG, an HPAEC-PAD analysis was conducted on VLM-SBG hydrolysate and compared with the VLM-SBG starting batch. This result, displayed in figure 12, show a disperse oligomer solution starting from single monomers to oligomers with DP ~25. A small signal at 80 min indicates that oligomers of higher DP is present as well. Additionally, the small signals observed between the high signals represent oligomers with a hydrodynamic volume grater/less than the two neighboring signals. The determination of the oligomers was done based on a standard of laminaran solution containing oligomers of DP 2 to DP 6.

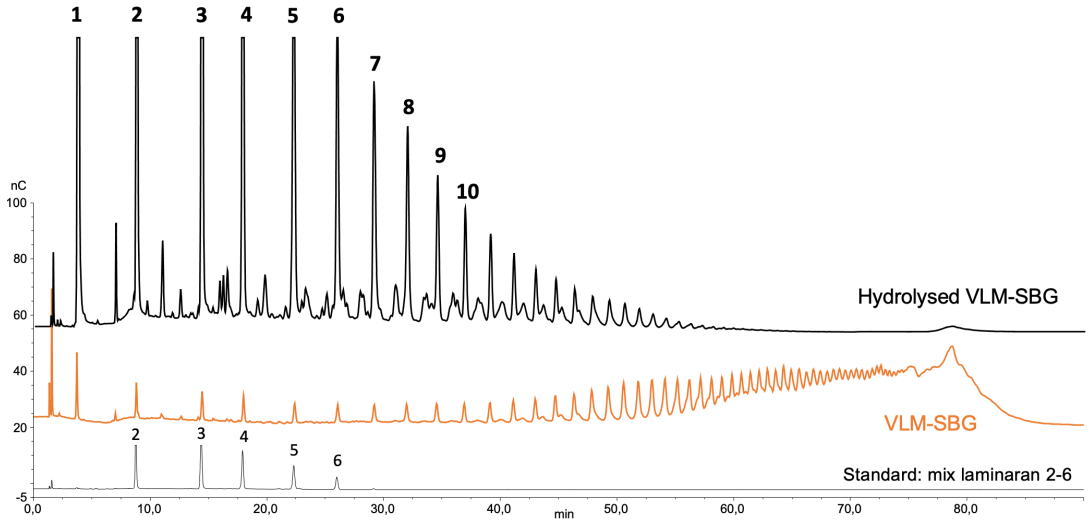

Figure 12: HPAEC-PAD chromatography of VLM-SBG starting batch compared to VLM-SBG hydrolysate (5mg/ml, 99°C, 75 min, 0.1M H_2SO_4). Standard: mixed laminaran solution (DP 2-6)

Figure 13 depicts the ^{1}H-NMR spectra of the hydrolysed VLM-SBG with a polydisperse distribution, that has been purified through dialysis (3.5 kDa). Based on the findings of Freimund *et al.* [60] and Hiroyuki *et al.* [61], the peak assignment was determined. Using equation 2, the average DP for the dialysed, SBG hydrolysate was

calculated to be DP = 9. An ^{1}H-NMR of a non-purified, SBG hydrolysate was also conducted for comparison and determination of average DP. The spectra is given in Figure B.1, and resulted in an average DP of 5 when including the free monomers. Without the free monomer, the average DP was 7.

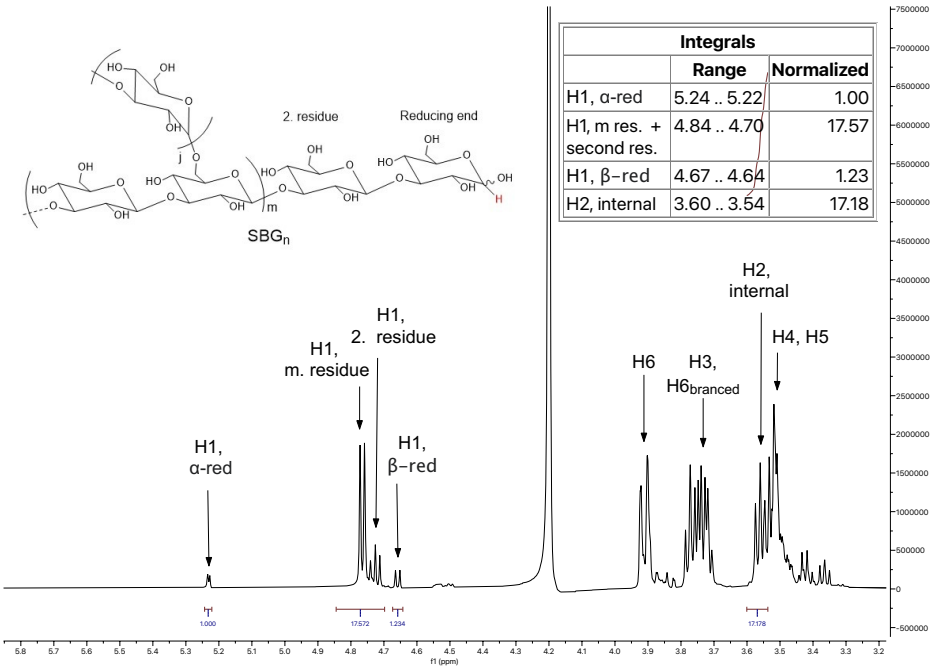

Figure 13: ^{1}H-NMR spectra of hydrolysed, dialyzed (3.5 kDa) and non-fractionated VLM-SBG at 82°C in D_2O. Recorded at 600 MHz. Number of scans, NS: 128. Average DP = 9. General structure of SBG is included, along with table containing the integrals of interest in calculation of DP.

4.1.2 Differences in solubility of batch 221-7 and VLM-SBG

Assuming a random degradation of the SBG batches, possible differences in chain lengths of batch 221-7 and VLM-SBG were seen as insignificant. However, during implementation, a difference in solubility between batch 221-7 and VLM-SBG was observed both prior and after degradation. As seen in figure 14, the start batch of VLM-SBG is fully dissolved in MQ giving a clear solution. Batch 221-7 on the other hand did not dissolve in MQ resulting in a cloudy solution. Possible reasons batch 221-7 not dissolving in MQ is due to aggregation, and different solvents were tested to evaluate its solubility.

Table 1: Solubility of hydrolysed and starting batch of 221-7 compared to hydroysed (5mg/ml, 99°C, 75 min, 0.1M H_2SO_4) and starting batch of VLM-SBG, in different solvents and/or conditions.

	221-7 SBG		VLM-SBG	
	Batch	Hydrolysed	Batch	Hydrolysed
MQ, RT	Insoluble	Insoluble	Soluble	Soluble
MQ, 99 °C	Soluble	Soluble	Soluble	Soluble
DMSO, RT	Soluble	Soluble	Soluble	Soluble

As seen in table 1, VLM-SBG was soluble in all four cases. On the contritely, the batch of 221-7 SBG and hydrolysed 221-7 was not soluble in MQ at RT. Neither did an increase of pH through addition of NaOH in RT result in dissolution of the two samples. However, by increasing the temperature to 99 °C both samples dissolved. To preserve a such high temperature during analysis and reaction is difficult. A different solvent that can dissolve 221-7 in RT was of interest. As seen in both figure 14b and table 1, using DMSO as solvent resulted in clear solution at RT for both hydrolysed 221-7 and batch 221-7. This results enables further analysis such as ^{1}H-NMR to investigate the reasons for 221-7 not to dissolve in solvents where VLM-SBG dissolves.

(a) **(b)**

Figure 14: **(a)** Comparison of SBG hydrolysate (5 mg/ml) from batch 221-7 and VLM, neutralized to pH 7. **(b)** Hydrolysed SBG from batch 221-7 (30mg, ~ 70% Na_2SO_4) dissolved in DMSO (2 ml) and MQ (2 ml).

4.2 Desalting methods for SBG oligomers

Following preparation of the desired SBG oligomer distribution, the sample is purified prior to conjugation as SBG hydrolysate contains a relatively high amount of salt (~ 70 wt.%). Two different desalting methods were conducted to find an optimal purification method. This is of interest since the purification steps are highly time-consuming and tend to lead to a significant loss of mass, especially polysaccharides containing only a few residues.

4.2.1 Desalting with dialysis

In order to determine the relationship between salt-removal and time at different cut-offs, the most commonly used 3.5 kDa cut-off was compared to a 100-500 Da cut-off. Two samples of freeze-dried SBG hydrolysate (7 mg) was prepared and filled in each dialysis bag. The graph shown in Figure 15 show that the salt concentration in dialysis bag decreases more rapidly during dialysis aginst MG compared to 0.05 M NaCl. It also show that a lower salt concentration is obtained in the 3.5 kDa dialysis after 30 hours, and that the concentration is about the same after 70 hours.

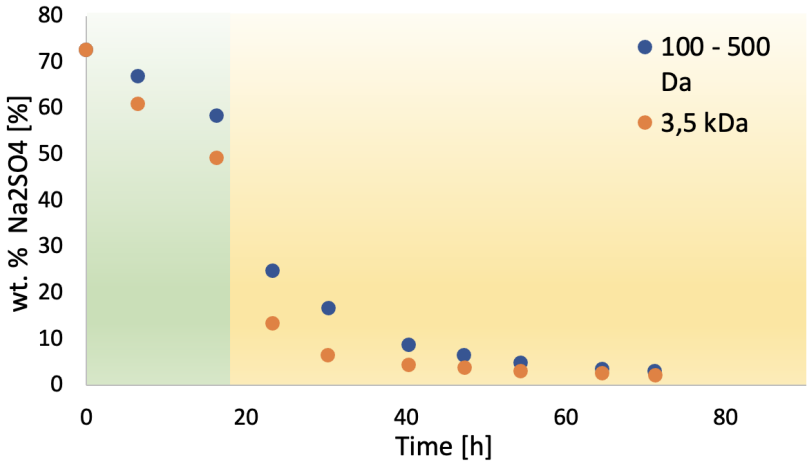

Figure 15: Graph showing Na_2SO_4 concentration in SBG hydrolysate using a 100 - 500 Da dialysis compared to 3.5 kDa dialyis. At shift was conucted at each measurment. Green area represent dialysis against 0.05M NaCl, while in yellow the samples were dialysed against MQ.

Two samples of freeze-dried SBG hydrolysate (7 mg) was prepared and filled in each dialysis bag. The graph shown in Figure 15 show that the salt concentration in dialysis bag decreases more rapidly during dialysis aginst MG compared to 0.05 M NaCl. It also show that a lower salt concentration is obtained in the 3.5 kDa dialysis after 30 hours, and that the concentration is about the same after 70 hours.

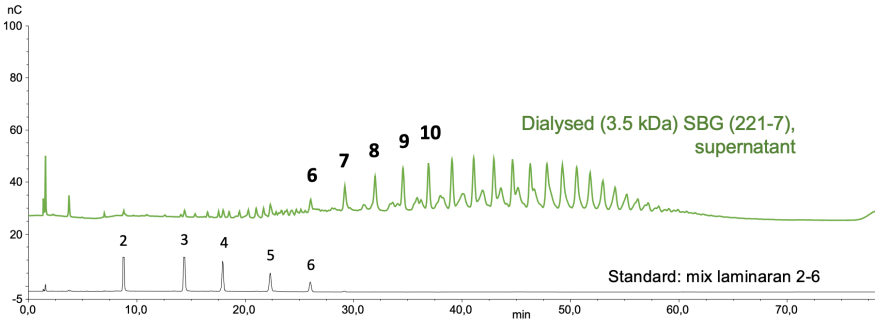

Figure 16: HPAEC-PAD analysis of SBG hydrolysate dialysed with 3.5 kDa.

A HPAEC-PAD analysis was conducted on the sample with 3.5 kDa dialysis bag, to determine the distribution of oligomers after dialysis. The result indicated that oligomers with DP < 6 is not significantly present in the solution.

4.2.2 Desalting with Centricon filtration

Due to purification with dialysis being a slow, finding an alternative desalting method is of great interest. Thus, an analysis was conducted using centricon centrifugal filtration. This method uses a 3.5 kDa filter and requires much less time, as well as easy to use when handling larger volumes.

Thinking that this method could be good alternative to dialysis, the centrifugal filtration of SBG resulted in a high accumulation (Figure C.3) of substance on the filters, most likely due to the high concentration of SBG. The aim of this technique was to separate minor impurities such as salt with the oligomers, an a HPAEC-PAD analysis of both retante and filtrate was conducted to see if SBG is permeate through the filter. Additionally, an NMR analysis was performed to calculate average DP. Seeing that both the HPAEC-PAD and NMR analysis resulted in exceedingly similar results between the filtrate and the retentate, indicates that oligomers are

not preserved in the filter during a such centrifugal filtration.

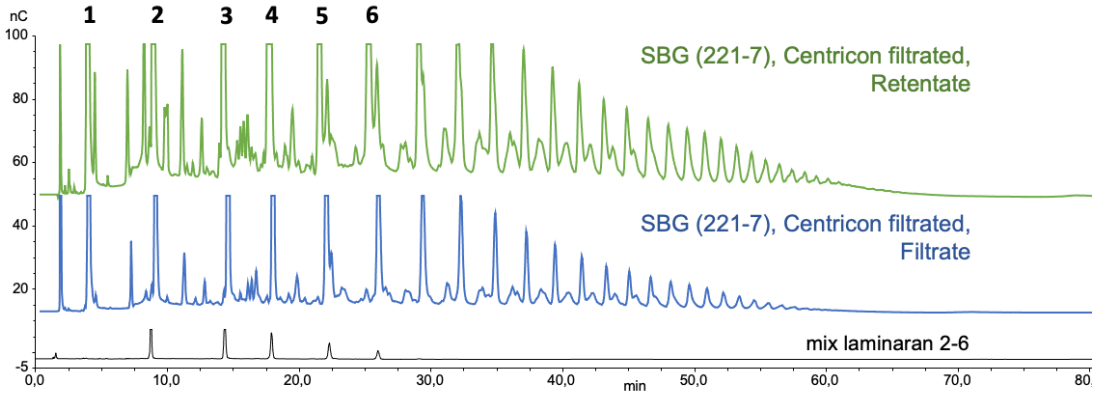

(a)

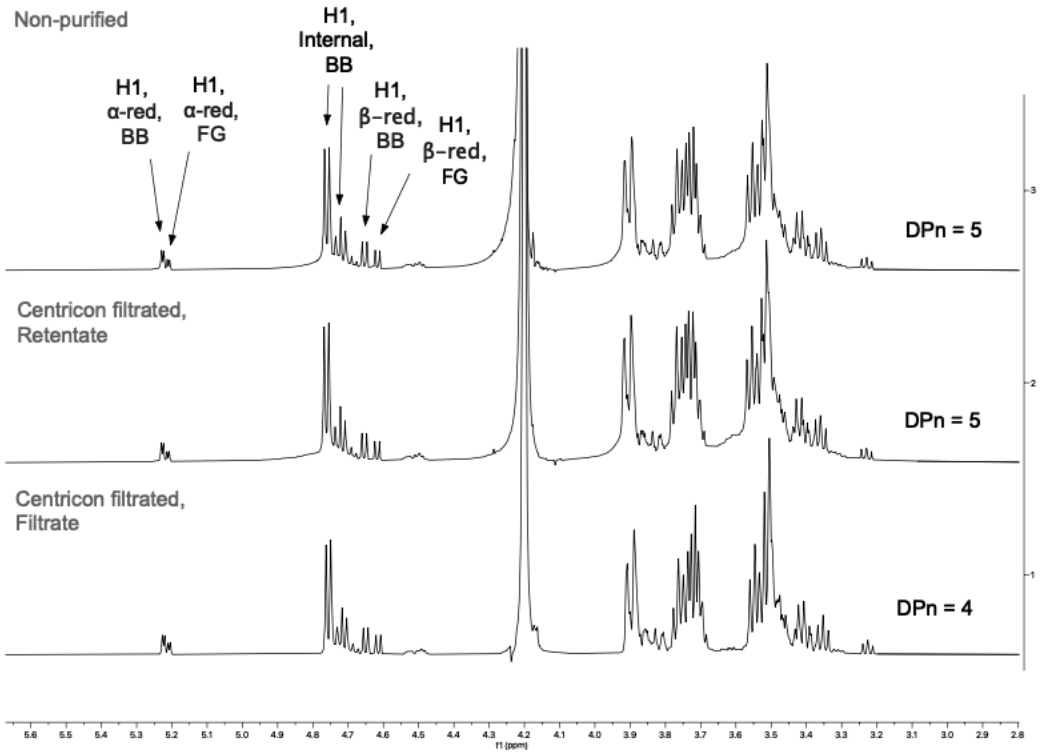

(b) SBG (221-7) hydrolysate

Figure 17: a) HPAEC-PAD analysis of retentate and filtrate from centrifugal filtration of hydrolysed SBG (221-7). **a)** ^{1}H-NMR spectra of non-purified SBG (221-7) hydrolysate (top), retentate (middle) and filtrate (bottom) from centrifugal filtration. BB = Backbone. FG = Free glucose.

4.3 Preparation of PDHA activated SBG

In the aimed preparation of SBG_m-b-chitosan, the initial step was to activate SBG_m with PDHA linker molecule. I.V. Mo reported in her doctoral theses [3] a protocol for a such conjugation, using a fractionated SBG_5 solution. However, a protocol for direct activation of the polydisperse SBG hydrolysate, meaning a oligomer distribution of DP 1 - 25, has not jet been reported. SBG_m was conjugated as described in Section 4.3.1, using 10 equivalents of PDHA. Two parallel conjugations were conducted. One in which the SBG hydrolysate was purified (3.5 kDa dialysis) prior to conjugation, and the other as direct SBG hydrolysate (containing a relatively high amount of salt). This was of interest due to the possibility to reduce preparation time and loss of mass in the final product.

4.3.1 Terminal conjugation of SBG_m-PDHA, using time-course ^{1}H-NMR

A ^{1}H-NMR time-course analysis of terminal of SBG with PDHA was performed on a purified (Figure 18) and a non-purified (Figure D.4) SBG hydrolysate. This resulted in a successful preparation of SBG=PDHA in both instances. The reaction is validated by the observation of increasing chemical shifts at 7.6 ppm ((E)-oxime), 7.0 ppm ((Z)-oxime) and 4.3 ppm (N-pyranoside), and the decrease in α- (5.2 ppm) and β- (4.6 ppm) reducing ends. The kinetics analysis (Table 2) from time-course analysis resulted in a combined yield of 91% and 81% for purified and non-purified SBG hydrolysate, respectively. Both reactions occurring quickly having a $t_{0.5}$ at 6.78 for purified and 6.72 for non-purified.

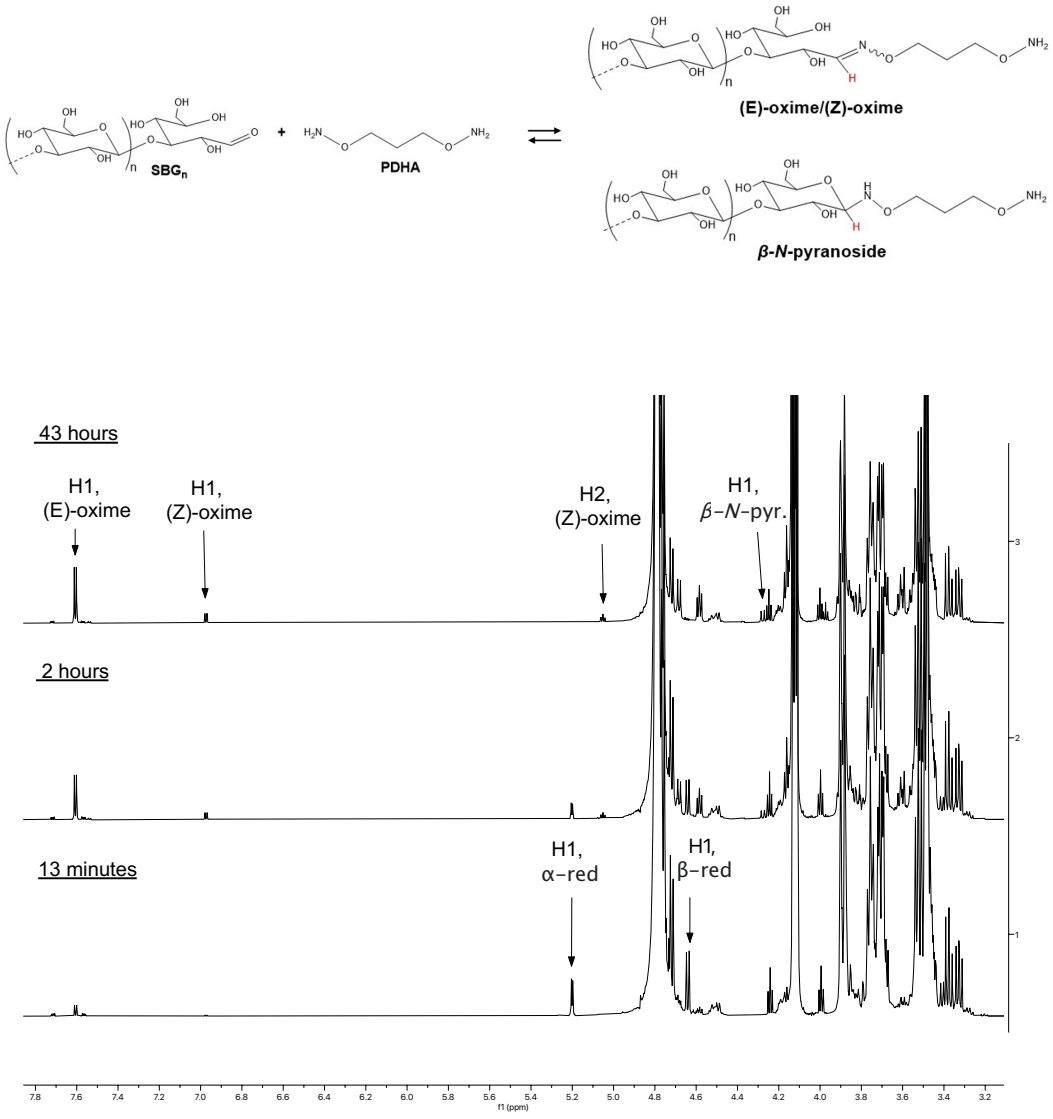

Figure 18: Terminal conjugation of purified (dialysed 3.5 kDa) SBG$_m$ oligomer solution with PDHA (10x equivalents) at RT (500mM NaAc, pH 4. Chemical structure (top) of reaction forming (E)-/(Z)-oximes and β-N-pyranoside in equilibrium. The respective hydrogens are shown in red.

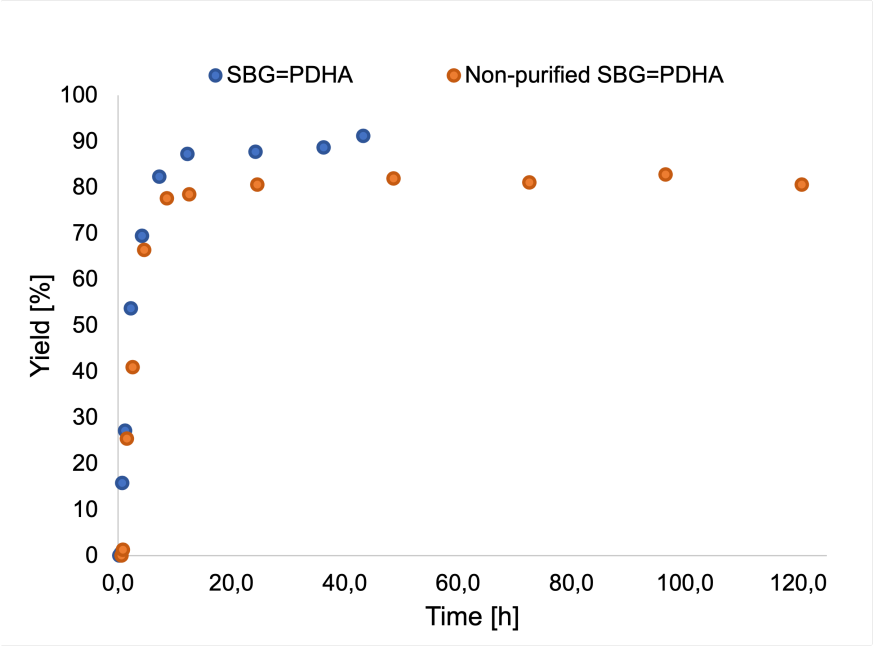

Figure 19: Graph showing the conjugation yield of SBG$_m$=PDHA of a priorly purified SBG hydrolysate compared to a non-purified SBG hydrolysate.

Table 2: Kinetics data PDHA activation of non-purified and purified (dialysis, 3.5 kDa) SBG hydrolysate (10mM, RT, pH 4). The model is provided by Professor Bjørn E. Christensen at Department of Biotechnology and Food Science, NTNU.

					A + B ↔ E		A + B ↔ Z		Combined
A	B	A/B [equi.]	$t_{0.5}$ [h]	$t_{0.9}$ [h]	k_1 [h^{-1}]	k_{-1} [h^{-1}]	k_2 [h^{-1}]	k_{-2} [h^{-1}]	equilibrium yield [%]
Purified SBG$_m$	PDHA	1:10	0.66	6.78	$1.7x10^{-2}$	$1.8x10^{-2}$	$2.3x10^{-3}$	$8.0x10^{-2}$	91
Non-purified SBG$_m$	PDHA	1:$\lesssim$ 10	0.72	6.72	$1.4x10^{-2}$	$1.0x10^{-3}$	$2.5x10^{-3}$	$3.1x10^{-1}$	80

4.3.2 Reduction and characterisation

To stabilise the activated SBG$_m$=PDHA oligomers for further use, α-picoline borane was added to the conjugate solution for reduction creating secondary amines. This reaction occurs at 40°C, and was therefore not analysed through time-course NMR. Instead, a NMR analysis of separated and purified SBG$_m$-PDHA was taken to validate reduction. Size-exclusive chromatography (SEC) (Figure **??**) was used to separated the different chain lengths of the reduced SBG$_m$-PDHA oligomers.

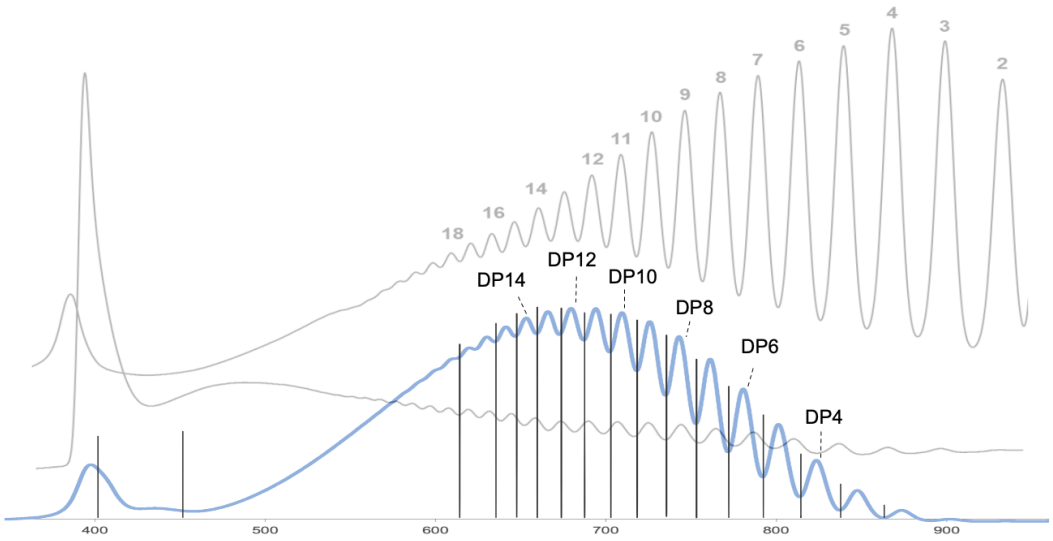

Figure 20: SEC chromatography of SBG$_m$-PDHA (blue) compared with SBG oligomers (grey). The chromatography of SBG oligomers is collected from the doctoral theses of I.V. Mo [3].

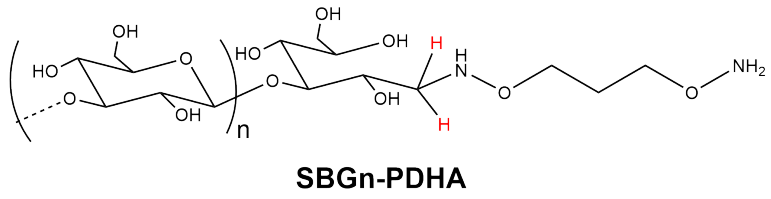

SBGn-PDHA

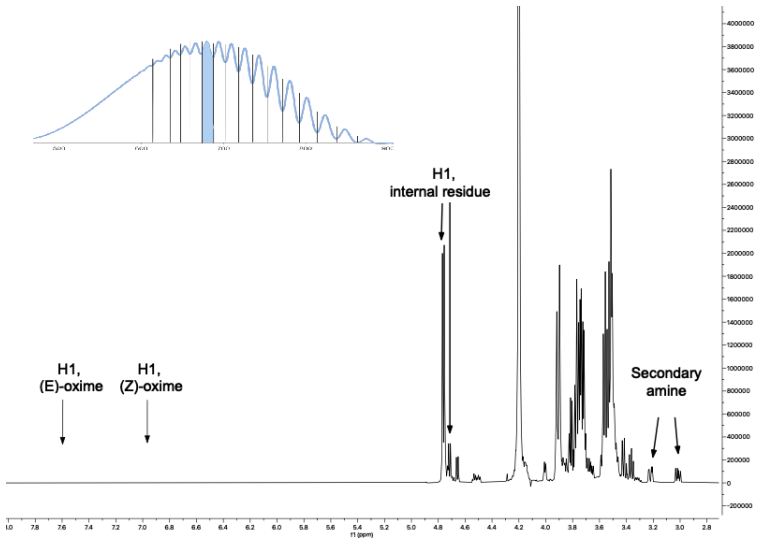

Figure 21: ^{1}H-NMR spectra with structure of reduced SBG$_{12}$-PDHA. The hydrogen in secondary amine is marked in red in the structure, indicating reduction.

The NMR spectra shown i22 of reduced and purified SBG-PDHA indicated high reaction yield as now chemical shifts of (E)- and (Z)-oximes as well as distinct peak for secondary amines are to be observed. The DP was determined by comparing integral area of internal residues with the area of secondary amines.

4.4 SBG_{10}-PDHA=$D_{11}M$ diblocks

One of the three main aims of this master's thesis was to prepare SBG_m-PEG_3-MD_n diblocks. The prepared, purified and fractionated SBG_{10}-PDHA oligomer were conjugated with in-house $D_{11}M$, using a protocol inspired by a preparative protocol for conjugating M-units with PDHA[6].

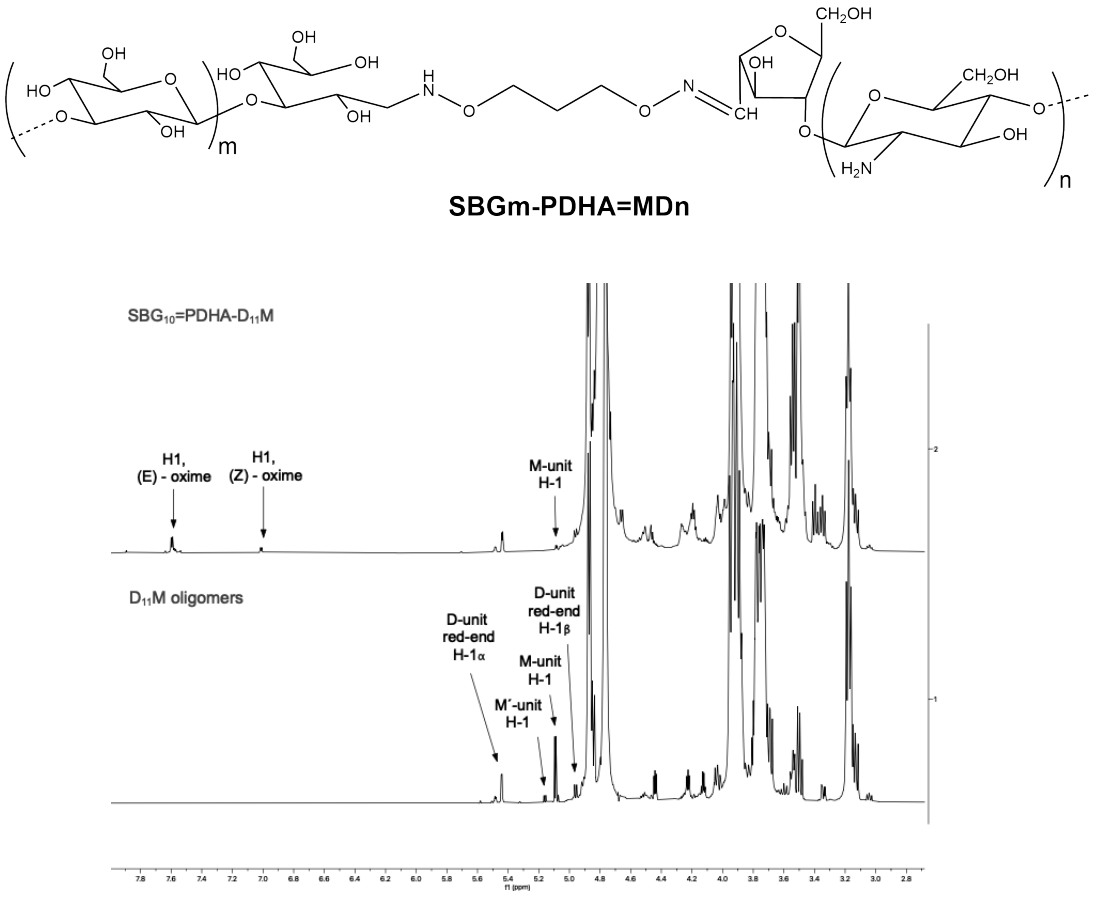

Figure 22: ^{1}H-NMR spectra of in-house $D_{11}M$ (bottom) and SBG_{10}-PDHA=MD_{11} after 13 minutes conjugation (7 mM, 1:1 [Equi.] (M-unit), RT, pH = 4). Formation of (E)-/(Z)-oximes, and reduction in M and M' peaks indicates a high reaction rate.

The time-course analysis of the conjugated showed significant peaks of (E)- and (Z)-oximes already a first spectra (13 minutes after mixture). When comparing it to a spectra of pure $D_{110}M$, the chemical shifts for M-unit reducing ends are clearly reduced. It is also observed little to no reduction in the chemical shifts of D-unit reducing end. The graph of conjugation yield plotted against time (Figure 23a) for the SBG-PDHA=MD_{11} diblock conjugation resembles the one of A_2M=PDHA conducted by I.V. Mo (Figure 23b) labeled in black.

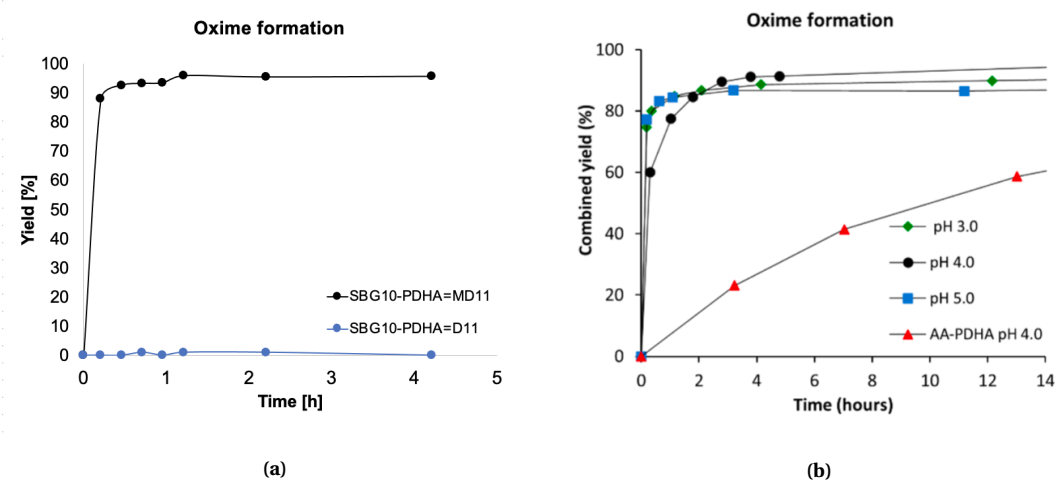

Figure 23: Combined yield for **a)** conjugation of SBG_{10}-PDHA=MD_{11} (7mM, 1:1 [Equi.] (M-unit), RT pH 4) compared to **b)** conjugation of A_2M=PDHA (20.1 mM, 1:2 [Equi.]), collected for I.V. Mo's doctoral theses [6].

4.5 SBG_m-PEG_3-Biotin diblocks

Significant loss of mass of SBG4-PEG-Biotin, most likely during dialysis required to remove the reducing agent (PB). With a cut-off of 3.5 kDa,the flexibility of PEG linker seems to result in a lower hydrodynamic volume of the diblock, resulting in SBG4-PEG-Biotin diffusing out.

4.5.1 Terminal conjugation of SBG_m=PEG_3-Biotin, using time-course ^{1}H-NMR

The third part of this master's thesis included optimising the preparative protocol, from the related specialisation project during fall of 2021, for SBG-b-biotin diblock and additionally transferring this protocol into SBG_m oligomers of other DP.

In preparation of SBG_4=PEG_3-Biotin, three reactions were conducted. Two of them (sample 1 and 2) having the exact same reaction conditions (2x equivalents of Biotin-PEG_3) to evaluate the repeatability of the reaction, and one with increased equivalent (4x equivalents of SBG_4) with an aim to increase the yield.

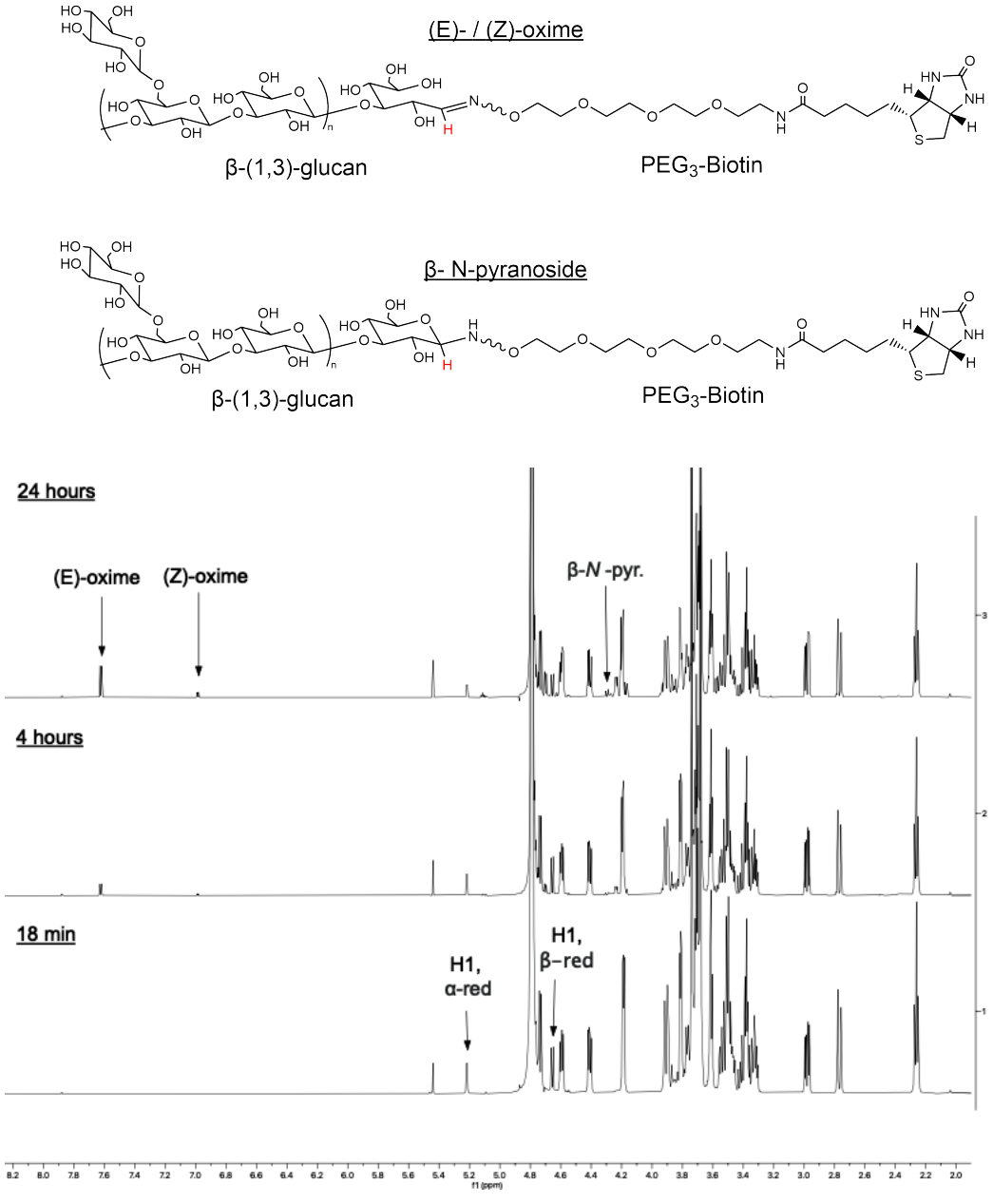

Figure 24: Time-course ^{1}H-NMR of conjugation of SBG_4=PEG_3-Biotin (10mM, 1:2 [eqiu], RT, pH 4), observing formation of (E)- / (Z)-oximes and β-N-pyranoside indication conjugation. The different hydrogens for the three structures are marked in red.

In preparation of SBG_4=PEG_3-Biotin, three reactions were conducted. Two of them (sample 1 and 2) having the exact same reaction conditions (2x equivalents of Biotin-PEG_3) to evaluate the repeatability of the reaction, and one with increased equivalent (4x equivalents of SBG_4) with an aim to increase the yield. This resulted in a yield of 59% for both sample 1 and 2 (1:2 [eqiv.]) and 74% for the increased equivalent (4:1 [eqiv.]), presented in figure 25b. The results from the kinetic analysis is presented in table 3.

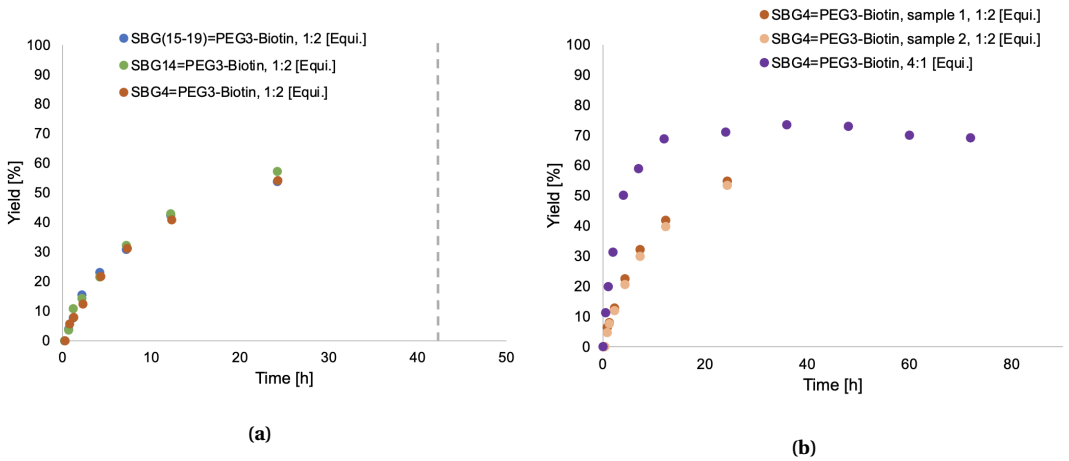

Figure 25: SBG_n=PEG_3-biotin conjugation. **a)** The gray dotted line represent at what time the were reduced, indicating a slightly higher final yield than given in the sample at 24h. SBG_4=PEG_3-Biotin corresponds to the average between sample 1 and 2. **a)** Comparison of yield obtained from conjugation of SBG_4=PEG_3-Biotin, with 2x equivalents of Biotin-PEG_3 and 4x equivalents of SBG_4. Sample 1 and 2 (1:2 [Equi.]) have equal reaction conditions.

Table 3: Kinetics data obtained from modelling of the conjugation (amination) of SBG_4 (10.0 mM/40 mM), SBG_{14} (10.0 mM) and SBG_{15-19} (10.0 mM) with PEG_3-Biotin at pH = 4, RT. The model is provided by Professor Bjørn E. Christensen at Department of Biotechnology and Food Science, NTNU.

					A + B ↔ E		A + B ↔ Z		Combined
A	B	A/B [equi.]	$t_{0.5}$ [h]	$t_{0.9}$ [h]	k_1 [h^{-1}]	k_{-1} [h^{-1}]	k_2 [h^{-1}]	k_{-2} [h^{-1}]	equilibrium yield [%]
SBG_4 (1)	PEG_3-Biotin	1:2	2.58	21.54	$3.1x10^{-3}$	$2.5x10^{-2}$	$2.0x10^{-4}$	$1.5x10^{-1}$	59
SBG_4 (2)	PEG_3-Biotin	1:2	2.7	23.16	$2.9x10^{-3}$	$2.2x10^{-2}$	$1.96x10^{-4}$	$1.5x10^{-1}$	59
SBG_{14}	PEG_3-Biotin	1:2	2.76	23.64	$3.1x10^{-3}$	$1.3x10^{-2}$	$2.0x10^{-4}$	$1.7x10^{-1}$	63
SBG_{15-19}	PEG_3-Biotin	1:2	2.64	22.38	$3.0x10^{-3}$	$2.0x10^{-2}$	$2.0x10^{-4}$	$1.7x10^{-1}$	59

4.5.2 Imine reduction of SBG_m=PEG_3-Biotin

In order to stabilise the formed SBG_m=PEG_3-biotin linkage, a reduction using PB was conducted. Previous analysis of reduction of this exact linkage[7] has shown a relatively low reduction rate, and an optimisation of the reported protocol was conducted (Section 3.9.1).

The estimated reduction yield for SBG_4-PEG_3=biotin, SBG_{14}-PEG_3=biotin and SBG_{15-19}-PEG_3=biotin is 62%, 70% and 83%, respectively (Table 4). The kinetics data of SBG_m-PEG_3=biotin conjugation was used to estimate the conjugation yield at time of reduction (41h/45h). This yield was then used to calculate the area of (E)-oximes at initiation of reduction (41h/45h). By estimating this area, the yield could be calculated through comparing area of (E)-oxime before and after reduction.

Table 4: Reduction yield for SBG_4-PEG_3-biotin, SBG_{14}-PEG_3-biotin and SBG_{15-19}-PEG_3-biotin, 10 equivalents PB for 124h at 40°C.

Diblock	Combined reduction yield [%]
SBG_4-PEG_3-biotin	62
SBG_{14}-PEG_3-biotin	70
SBG_{15-19}-PEG_3-biotin	83

4.5.3 Characterisation and purification of SBG_m-PEG_3-Biotin

A final conjugation and purification was conducted to removal excess PB and salt from the buffer solution, before shipping the SBG-b-biotin diblocks to Vienna for further analysis on cell responses. It was purified using 3.5 kDa dialysis prior to separating the conjugated diblock with the non-conjugated SBG and biotin using SEC. The chromatography of SBG_4-PEG_3-biotin, SBG_{14}-PEG_3-biotin and SBG_{15-19}-PEG_3-biotin is displayed in Figure 26 with a chromatography of a polydisperse SBG oligomer solution[3].

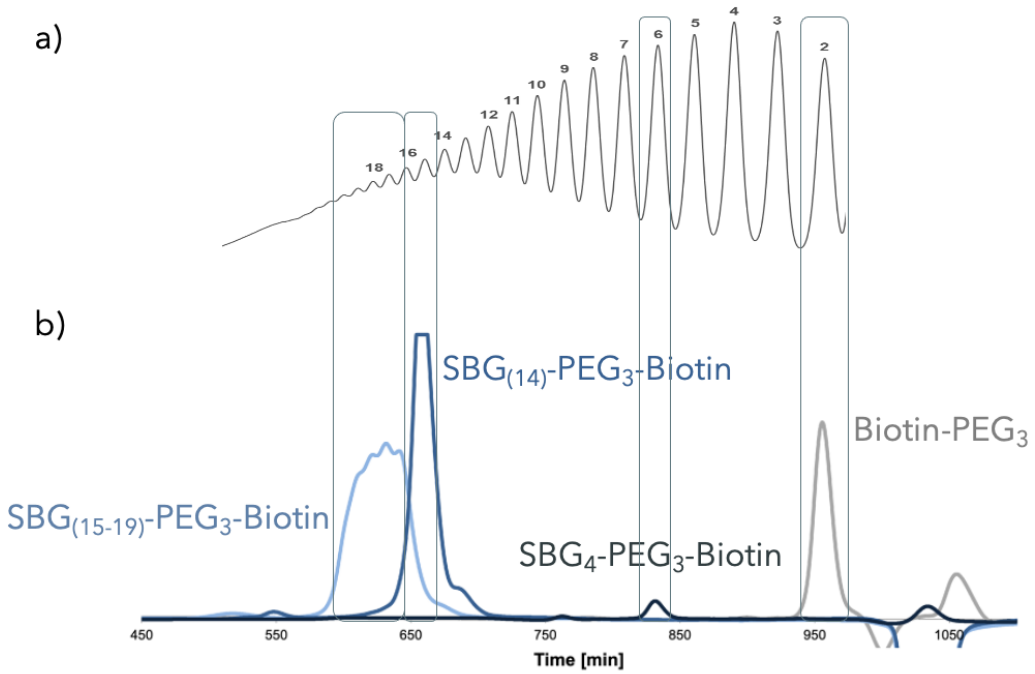

Figure 26: a) SEC chromatogram of hydrolysed VLM-SBG (5 mg/ml, 0.1 M H_2SO_4, 99°C, 75 min), conducted by I.V. Mo. [3],*p.68*. **b)** SEC chromatogram of SBG_m-PEG_3-Biotin after conjugation, reduction and dialysis with 3.5 kDa cut-off. The chromatogram of pure Biotin-PEG_3 is collected from the related specialisation project during fall of 2021 [7]

The NMR analysis (Figure 27) validates e relatively high reduction since the chemical shifts of (E)-/(Z)-oximes are nearly gone, and a formation of secondary amines between the SBG and PEG is visible. With these promising results, the final amount of theoretical mass (Table 5) is a drawback most likely caused by loss of mass during purification and dialysis, especially in the case of SBG_4. What is to be observed is that the total mass was much higher than the theoretical mass, most likely due to dialysis being terminated after 3x shifts in an attempt to preserve as much product as possible.

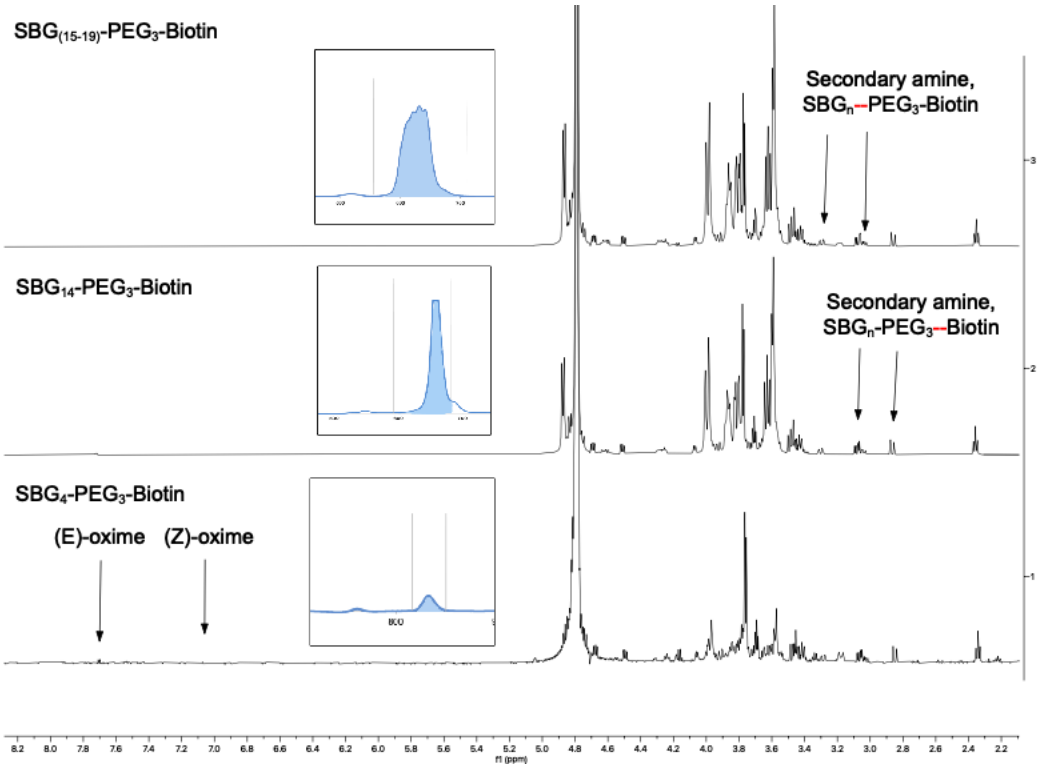

Figure 27: ^{1}H-NMR characterization of reduced and purified SBG_4-PEG_3-Biotin, SBG_{14}-PEG_3-Biotin and SBG_{15-19}-PEG_3-Biotin, conjugated with 2 equivalents PEG_3-Biotin and reduced with 10 equivalents PB for 124h at 40°C.

Table 5: Mass of SBG_4-PEG_3-Biotin, SBG_{14}-PEG_3-Biotin and SBG_{15-19}-PEG_3-Biotin after conjugation (10mM, 1:2 [Equi.], pH 4, RT, 41/45h)), reduction (20x PB, 40 °C, 124h) and purification (3.5 kDa dialysis; 2 shifts, and SEC). The theoretical mass is calculated by comparing the known injection mass and the area of the biotin-PEG_3 chromatogram to the area of the diblocks.

Diblock	Theoretical mass [mg]	Total mass [mg]
SBG_4-PEG_3-Biotin	0.2	14.2
SBG_{14}-PEG_3-Biotin	4.1	39.2
SBG_{15-19}-PEG_3-Biotin	5.6	61.9

5 Discussion

This master's thesis aimed to prepare SBG oligomers for upcoming preparation SBG_m-b-chitosan SBG_m-b-biotin diblocks. Preparation, analysis, and purification of SBG oligomers constitutes the initial step for the two diblocks. In preparation of SBG_m-b-chitosan diblocks, activation of SBG_m-PDHA (PDHA = linker) was priory conducted, looking at the activation of purified and non-purified SBG_m hydrolysate solution. In the related specialisation project [7], a protocol for SBG-b-biotin preparation was developed, and optimised in the present thesis. Three different chain lengths of SBG_m-b-biotin was prepared.

5.1 SBG oligomer preparation and characterisation

5.1.1 Acid hydrolysis of SBG

Low molecular SBG 221-7/VLM-SBG) were degraded by acid hydrolysis (Section 3.5.1) to achieve oligomers with an average DP of approximately 10. This was desired because working with shorter chain lengths is more ideal in working with kinetics data by NMR, as well as involving fewer complications regarding solubility and other solution properties [10].

Following degradation, an HPAEC-PAD analysis (Figure 12) was conducted on hydrolysed VLM-SBG and compared with the starting batch of VLM-SBG. Corresponding with the expectations based on previous data [3] of such degradation, the chain length distribution of oligomers in the hydrolysed SBG was from DP 1 to DP $\sim$ 25. The small signals observed in between is likely due to branched oligomers as their hydrodynamic volume is grater than non-branched oligomers of the same main chain length [48]. However, further analysis is required for validation, for instance by ^{H}-NMR and calculation of the degree of branching. The batch of VLM-SBG clearly consist of SBG with longer chain lengths, as the signal increases with increased time. Signals for possible branching points is not observed in the VLM-SBG indicating a less disperse solution.

The ^{1}H-NMR spectra of non-purified, SBG hydrolysate is displayed in Figure B.1. Comparing this spectra with the spectra of purified SBG hydrolysate (Figure 13),

double peaks at the α- and β-reducing ends were solely observed in the non-purified. Based on previous data [8] these double peaks are most likely due to the presence of free monomers, as the chemical shifts for their reducing occurs at a slightly lower ppm than the reducing end on dimers, trimers, etc. In the purified NMR spectra, chemical shifts for such free monomers are not present, which corresponds with the expectations as their small hydrodynamic volume results in removal during purification. The average DP of the non-purified, SBG hydrolysate was calculated to be DP 5 when including these free monomers. Since the peaks for the reducing ends in the free monomers are readily distinguished, the solution contains a relatively high proportion of free monomers. In addition, the average DP rises from DP 5 to DP 7 if these free monomers are excluded from the calculation, revealing the specifics.

5.1.2 Differences in solubility of batch 221-7 and VLM-SBG

Acid hydrolysis of SBG was assumed to be random degradation, and possible differences in average chain length in batch 221-7 and VLM-SBG were seen as insignificant [24]. However, a few differences in 221-7 batch and VLM-SBG were observed both before and after degradation. Both 221-7 and VLM-SBG is retrieved from the same manufacturer, and should in principle be somewhat equal, they still showed a few differences. In solutes such as D_2O, VLM-SBG dissolved easily whilst batch 221-7 did not fully dissolve, leaving a cloudy solution (Figure 14a. The solubility of SBG is dependent of the degree of branching as well as chain length of the oligomers [48;24]. On the basis of this, it was anticipated that the solubility of batch 221-7 would increase after deterioration, which did not occur. A possible reason is presence of unbranched SBG oligomers, as they create a dense oligomer structures with low solubility [24;17]. Subsequently, as an attempt in characterising of the insoluble oligomers, finding proper solvent for batch 221-7 was of interest.

Working with polysaccharides, increasing the temperature will in most cases lead to an increased solubility [48], which corresponds with the result from batch 221-7 (Table 1). Knowing from reported work with SBG [17;11], DMSO is a well-known solvent in which SBG has proven solubility at much grater chain lengths than present study [32]. Thus, batch 221-7 was dissolved in both MQ and DMSO for comparison.

As seen in Figure 14b, it dissolved in DMSO which enables further analysis such as NMR-analysis, Dynamic Light scattering, SEC-MALLS, etc., to characterise these oligomers.

5.2 Desalting methods for SBG oligomers

5.2.1 Desalting with dialysis

Dialysis is a desalting and purification procedure that is both time-consuming and limited with respect to the preservation of small molecules. According to the HPAEC-PAD chromatography of the 3.5 kDa dialysis, peaks of oligomers with chain length < DP 6 are not significantly present, indicating being lost during dialysis. Since monomers, dimers, trimers, etc. have a small hydrodynamic volume, and consequently a relatively high diffusion rate through the membrane, the results are consistent with expectations. Thus, working with low molecular weight polymers, it has been observed a significant loss of mass during dialysis due to membrane diffusion. To minimize this loss, the dialysis cut-off can be decreased. However, a such reduction also leads to an increased time in the removal of salt and contamination.

As seen in figure 15, the 3.5 kDa dialysis bag has initially a higher efficiency in salt removal compared to the 100-500 Da dialysis bag, decreasing to 60 % and 66 % after 16 hours, respectively. It is also observed that both dialysis bags have a higher reduction rate when dialysis against MQ compared to against 0.05M NaCl. This corresponds with the expectations considering that the concentration gradient between outside and inside of dialysis is grater when dialysis against MQ compared to 0.05M NaCl. If requesting a highly purified product, the choice of cut-off in regard of time to achieve such low percentage of salt (e.g < 5 wt.%) the is, based on this analysis, insignificant. This is also due to to the driving force for diffusion of salt through the membrane, as a lower concentration gradient leads to less salt diffusing through membrane. Thus, the 100-500 Da dialysis bag will catch up with the 3.5 kDa bag due to higher concentration gradient. However, if the product does not have to be fully purified, the 3.5 kDa dialysis bag is more efficient.

The choice of cut-off in dialysis determines what molecular weight for spherical

polymers that is preserved during dialysis. Meaning, polymers with a minor molecular weight can diffuse, but are sometimes still preserved due to an the extensive structure (e.g linear).

5.2.2 Desalting with Centricon filtration

A new method for desalting and purifying the SBG_m hydrolysate, is the centrifugal (centricon) filtration. The method in it self is a lot less time-consuming than average dialysis, and easier to handle at lager volumes. For a future up-scaling of SBG preparation this centrifugal method could be a good option for purification.

However, the results on the centrifugal filtration of SBG_m did not turn our as promising as initially hoped for. As seen in Figure 17a, the SBG oligomer composition of retentate and filtrate are close to similar. This indicates that the oligomers is not preserved in the retentate, resulting in a high loss of mass as they permeates the filter-membrane. Additionally, the NMR-spectra of oligomers in retentate and filtrate was compared to a non-purified SBG hydrolysate (Figure 17b). Supporting the previous statement, the average DP was about the same in all three cases (DP $\sim$ 5), only slightly less in the filtrate solution (DP 4). Meaning that the proportion of penetrated oligomers relative to non-permeated oligomers is slightly higher for smaller oligomers than for larger oligomers. During implementation, an accumulation of mass on the filters was also observed (Figure C.3).

The primary purpose of this centrifugal filtering is to eliminate salt and minor impurities by allowing it to pass through the membrane while preserving the polymers. Given that the polymers in this analysis were not well conserved, it is not regarded as a viable purification method.

5.3 Preparation of PDHA activated SBG

5.3.1 Terminal conjugation of SBG_m=PDHA

The aim of the second part of the master's thesis was to prepare SBG_m-PDHA=MD_n diblocks, starting with PDHA activation of SBG_m. Polydisperse SBG hydrolysate was directly activated without being separated based on chain lengths prior to con-

jugation, which is commonly been conducted in reported studies [4;2;11;10].

A high concentration of salt such as NaCl, Na_2SO_4, etc. is assumed to not affect the reaction kinetics, but has not been directly analysed previously. To determine if a high salt content in the solution affects the reaction kinetics, an time-course analysis with 70 w/w% of Na_2SO_4 was conducted (non-purified SBG hydrolysate) and compared to a purified (3.5 kDa dialysis) SBG solution.

The NMR spectra from the time-course analysis of both purified (Figure 18) and non-purified (Figure B.1) showed increasing chemical shifts of (E)- and (Z)-oximes, as well as reducing in reducing ends, attributing conjugation. Comparing the purified SBG hydrolysate and the non-purified SBG hydrolysate, the conjugation yield was close to similar, 91% against 80% (Figure 19, respectively. This indicates that a high concentration of Na_2SO_4 does not significantly affect the conjugation rate. A high concentration of salt corresponds to high ionic strength (effects of ions in solution [62]). For negative charged polymers, a high ionic strength decrease the chain expansion, due to shielding by the salt. This could reduce the availability of the reducing end, decreasing reaction rate. However, since SBG is a neutral polysaccharide, the high salt concentration was assumed not affect the reaction kinetics.

What is to be observed, on the other hand, is the presence of double peaks at the (E)/(Z)-oximes in the non-purified NMR spectra (Figure B.1). Previous studies [8] show that these peaks most-likely correspond with (E)/(Z)-oximes of polymers and free glucose molecules. When analysing the conjugation of purified SBG hydrolysate compared to non-purified, the relevance of the free glucose's are of significance. During conjugation, the reducing ends of both polymers and free glucose molecules will be activated resulting in a high percentage of SBG_1=PDHA diblocks. In the non-purified solution, the average DP of the polydisperse SBG will be less compared to purified, due to loss of short-chained SBG < DP 6 during dialysis (see Section 4.2). When assuming same DP of purified and non-purified, the equivalents of the non-purified will be less, resulting in a decreased reaction rate [4]. The small difference in conjugation yield (Table 2) between purified and non-purified may therefore be a result of a slightly difference in equivalents of PDHA, instead of the high salt concentration itself.

5.3.2 Reduction and characterisation

Irreversible reduction of SBG$_m$=PDHA using PB as reducing agent was preformed to stabilisation. The chromatography (Figure 20) shows the wide distribution of the different chain lengths of SBG$_m$-PDHA oligomers. Compared to SEC conducted by I.V. Mo [3] on non-conjugated SBG$_m$, the oligomers of a certain DP are slightly larger in hydrodynamic volume than the corresponding SBG$_m$-PDHA. Seeing that PDHA is a small molecule (Figure **??**), this slightly increase in size indicates, together with the time-course analysis ^{1}H-NMR (Figure 18), that conjugation has occurred.

The reduction of the SBGm-PDHA oligomers was validated by ^{1}H-NMR analysis after separation and purification. The spectra, taken after – hours reduction with 10x PB, shows clear chemical shifts for secondary amines. That, along with no observed peak for the (E)-/(Z)-oximes, indicates a high obtained reduction yield. Reaction kinetics obtained from one pot reductive amination (activation and reduction, simultaneously) of SBG$_4$=PDHA [3] resulted in a yield of approximately 40% after 200 hours. Kinetics data from conjugation of SBG$_5$=PDHA in the same study reported a $t_{0.9}$ (time reaching 90% of equilibrium yield) at 7.1 hours, reaching a combined equilibrium yield at 94%. It was concluded that the reduction of SBG$_m$=PDHA was evidently slow, which contradicts the results of the present study. However, PDHA was added at a much higher equivalent (20x compared to 3x) which is known to increase reduction [4]. Additional research on the reduction of SBG$_m$-PDHA would provide a better understanding of the reduction kinetics.

5.4 SBG$_m$-PDHA=D$_n$M diblocks

With the aim of preparing SBG$_m$-PDHA=MD$_n$ diblocks, a preparative protocol was developed. On the basis of previous data regarding conjugation between M-units and PDHA [2;3], it was hypothesized that the following conjugation would result in approximately the same reaction kinetics using an equivalent protocol. This hypothesis was made on the premises that research indicates that the type of reducing ends has a significant impact on the kinetics of conjugation [10].

The high reactivity of both AnM and DnM has been proven, resulting in a conjuga-

tion yield of > 90% in less than 4 hours [6], as shown in Figure 23b collected from the doctoral theses of I.V. Mo. The result from the present activation of SBG_{10}-PDHA with $D_{11}M$ (Figure 23a showed the same conclusion, with a yield of 90% after less than 30 minutes. This indicated a high reproducibility of D_nM activation during equal reaction conditions. It also indicated that the increase in DP (from DP4 to DP 12) and the SBG residue does not effect the conjugation yield. I.V Mo also reported that the reducing ends of the D residues, was unaffected, corresponding to the SBG_{10}-PDHA=M_{11} activation. Thus, a low reactivity of the D-residues.

5.5 SBG_m-PEG_3-Biotin preparation and characterisation

5.5.1 Terminal conjugation of SBG_m=PEG_3-Biotin, using time-course ^{1}H-NMR

The last main part of the aim of this master's thesis was to prepare SBG-b-biotin diblock. Since the both of the purification methods used in preparation of SBG oligomers resulted in a high loss of SBG oligomer with chain length < DP 6, already prepared SBG_4 from Megazyme was used.

The previous analysis [7] of SBG_5=PEG_3-Biotin conjugation resulted in a combined yield of 60$ after 15 hours. However, the conjugation had not yet reached equilibrium, and in optimising the protocol, the conjugation time was increased to 48 hours. In the time-course NMR analysis, chemical shifts for (E)-/(Z)-oximes were observed along with reduction in reducing ends. Calculation of the combined yield, presented in Figure 25a, show that a DP < 20 for the SBG_m does not effect the conjugation rate, as all three resulted in a yield of approximately 60% (Table 3. This result is exactly equivalent to the data obtained from the related specialisation project.

Due to the current conjugation yield of SBG_m-b-biotin, an analysis of conjugation with increased equivalents was conducted on to determine if it resulted in a higher conjugation yield. Oligomers containing just a few residues are more favorable in kinetics analysis [10], and SBG_4-b-biotin was thereby studied. As seen in Figure 25b, the obtained combined equilibrium yield when increasing the equivalent from 2x to 4x was still around 60%. However, the reaction rate was much higher reaching equilibrium after about 10 hours. In addition, it was observed that reproducibility

was high when the same reaction conditions were used, as samples 1 and 2 of the 2x equilibrium were nearly identical.

5.5.2 Imine reduction of SBG_m=PEG_3-Biotin

Following conjugation, reduction of SBG-PEG_3-biotin was conducted. Knowing that this specific reduction was slow, the reduction was set to last for 5 days at 40°C. This resulted in a combined reduction yield of 62%, 70% and 83% for SBG_4-b-biotin, SBG_{14}-b-biotin and SBG_{15-19}-b-biotin, respectively, indicating that an increased reduction yield with increased chain length. This was not expected as previous data has shown that generally, an decrease in chain length increases the reduction yield. However, considering that this analysis was only conducted once with each chain length, further analysis is required to determine is this is exception.

5.5.3 Characterisation and purification of SBG_m-PEG_3-Biotin

After conjugation and reduction, the samples were dialysed with at cut-off of 3.5kDa. Figure 26 shows the chromatography of $SBG_{(15-19)}$-PEG_3-Biotin, SBG_{14}-PEG_3-Biotin and SBG_4-PEG_3-Biotin along with pure Biotin-PEG oxyamine. All three diblocks resulted in a left-displacement of two glucose-unit compared to pure SBG. Seeing that the hydrodynamic volume of Biotin is about equal to SBG_2, this displacement of the diblocks validated, along with the NMR spectra (Figure 27), diblock formation. No signal for Biotin-PEG_3 was detected in the chromatography either three of the diblock, due to removal of Biotin-PEG_3 during dialysis. This is because of its small hydrodynamic volume, also corresponding with the chromatography from the related specialisation project [7].

Knowing that 2 mg of Biotin-PEG_3 was injected into the SEC system, the theoretical mass of the diblocks could be calculated. This resulted in a theoretical mass of 5.6 mg, 4.1, mg and 0.2 mg of $SBG_{(15-19)}$-PEG_3-Biotin, SBG_{14}-PEG_3-Biotin and SBG_4-PEG_3-Biotin, respectively. Based on this, it is reasonable to conclude that a large quantity of SBG_4-PEG_3-Biotin is lost during dialysis of 3.5 kDa. Previous analysis, see Figure 16, show that SBG oligomer with a DP < 6 is significantly removed during

dialysis, corresponding with the high loss of mass of SBG_4-PEG_3-biotin. An alternative preparation method for $SBG_{(}4)$-PEG_3-Biotin diblock were therefor introduced. In this preparation, the diblock were not reduced after conjugation due to previous data[?] showing reasonable stability of the imine at pH near 7. Without the reducing step, removal of PB through dialysis is not necessary. The evaluation of which the salt from the buffer needs to be removed is dependent of the up-coming analysis. However, removal of only the salt required much less shifts and time, and thus less diblock diffuses through the dialysis bag resulting in higher yield. Using a smaller cut-off will increase the required time, but considering that salt is removed more rapidly than PB, this might be an decent solution.

5.6 Future perspectives

Preparation of SBG oligomers were partially successful during this master's thesis, as the purification step using centrifugal filtration was not seen as viable method and preserving oligomers of few residues still consist of difficulty. Exploring new possibilities in purifying SBG oligomers is therefore needed to obtain a increased mass of these small oligomers. Finding a more effective method is also desirable, particularly if these preparations are to be scaled up.

Further research on SBG-b-chiotsan would firstly be to analyse reduction kinetics to stabalise these block polysaccharides. Additionally, it would be interesting to analyse their solution properties and stability over time. Especially in regard of human environment as both of the polysaccharides consist of biochemical activity. As with SBG-b-biotin, optimize the preparative protocol in order to increase conjugation yield, and continue analyzing the cell response to diblocks with varying chain lengths. One could also conduct a dialysis analysis to determine the rate of biotin-PEG diffusion out of the dialysis bag when using 3.5 kDa. This would be useful in the purification and removal of all biotin in order to achieve the highest preservation of diblock, and then a clearer picture of how long dialysis must be conducted before nearly all non-conjugated biotin is removed.

Creating diblock polysaccharides made exclusively out of renewable resources would be a desired aim in the nearest future. Also, being able to terminally conjugate the non-reducing end of polysaccharides would open possibilities in preparing triblocks (ABC, ABA, etc.), and medical applications consisting of multiple different properties. Solberg *et el.* has reported success in preparing nanoparticles consisting of alginate-b-dextran diblocks [10]. Thus, it would be highly interesting to analyse the preparation of nanoparticles made out of other diblocks, such as SBG-b-Dextran or SBG-b-chitosan. If it were to succeed, a diversity of possibilities within nanotechnology and/or nano-medicine would be opened. This again would make diblock polysaccharide a highly interesting field in regard of future medicine and green chemistry.

5.7 Conclusion

This master's thesis consisted of three main parts including preparation and purification of SBG oligomers, and preparation of SBG-b-chitosan and SBG-b-biotin diblocks. The acid hydrolysis of SBG resulted in the desired distribution of oligomers between DP 1 to DP ~ 25. The purification analysis revealed that the choice of cut-off during dialysis has the greatest impact on salt removal when the sample does not require complete purification. In addition, the alternative centrifugal filtration method for purifying SBG oligomers was unsuccessful due to the oligomers permeating through the filter membrane.

The first step towards SBG_m-PDHA-MD_n diblock consisted of activating the SBG oligomers with PDHA. Aimed to reduce purification steps and decrease preparation time, direct activation of SBG hydrolysate was analysed. Due to the paucity of data, the effect of a high salt concentration during conjugation was also investigated. Purification of SBG hydrolysate via dialysis prior to being conjugated with PDHA were not concluded as a necessity since both resulted in a high conjugation yield of 80-90%. However, if the difference i DP between the purified and non-purified solution is not accounted for, the reaction equivalent will decrease in the non-purified if assming same DP as purified. This again will decrease the reaction yield and further analysis is necessary to conclude whether the small difference is due to the high concentration of salt concentration or decreased equivalent. The SBG_m-PDHA=MD_n was successfully prepared reaching a combined equilibrium at approximately 95% after 30 minutes.

The third part of this thesis aimed to prepare different SBG_m-PEG_3-biotin diblocks. Kinetics data from conjugation resulted in an obtained combined equilibrium yield of ~ 60% in all three chain lengths of SBG ($4 < DP < 20$). On the basis of these results, it was concluded that the chain length does not significantly influence the conjugation rate in cases where DP is under 20, but further investigation is necessary in cases with longer oligomers. The slightly increase in yield of reduction rate observed with increasing DP of SBG does not correspond to the expectations. A conclusion whether this trend is due to an exception can not be made bade on this single analysis. However, all three resulted in a relatively high reduction yield (60 -

80%).

The aimed preparation of SBG-b-chitosan and SBG-b-chitosan were achieved during this master's these. With this result, optimisations of protocols and purification methods can be done to obtain grater results in future research.

References

[1] Solmaz Bayati. Mixed block copolymer solutions: Self-assembly and interactions. 2016.

[2] Mina Gravdahl. *Preparation, characterization, and solution properties of chitosan-b- dextran diblocks*. NTNU, 2021. Master's thesis.

[3] Ingrid V. Mo. *Towards block polysaccharides: Terminal activation of chitin and chitosan oligosaccharides by dioxyamines and dihydrazides and the preparation of block structures*. NTNU Grafisk senter, 2021. ISBN 978-82-326-6212-8. Doctoral theses at NTNU, 2021:120.

[4] Ingrid Vikøren Mo, Yiming Feng, Marianne Øksnes Dalheim, Amalie Solberg, Finn L. Aachmann, Christophe Schatz, and Bjørn E. Christensen. Activation of enzymatically produced chitooligosaccharides by dioxyamines and dihydrazides. *Carbohydrate Polymers*, 232:115748, 2020. ISSN 0144-8617. doi: https://doi.org/10.1016/j.carbpol.2019.115748. URL `https://www.sciencedirect.com/science/article/pii/S014486171931416X`.

[5] Dongbin Yang, Weihong Zhang, Huanyun Zhang, Fengqiu Zhang, Lanmei Chen, Lixia Ma, Leon M. Larcher, Suxiang Chen, Nan Liu, Qingxia Zhao, Phuong H.L. Tran, Changying Chen, Rakesh N Veedu, and Tao Wang. Progress, opportunity, and perspective on exosome isolation - efforts for efficient exosome-based theranostics. *Theranostics*, 10:3684–3707, 2020. doi: 10.7150/thno.41580. URL `https://www.thno.org/v10p3684.htm`.

[6] Ingrid Vikøren Mo, Marianne Øksnes Dalheim, Finn L. Aachmann, Christophe Schatz, and Bjørn E. Christensen. 2,5-anhydro-d-mannose end-functionalized chitin oligomers activated by dioxyamines or dihydrazides as precursors of diblock oligosaccharides. *Biomacromolecules*, 21(7):2884–2895, 2020. doi: 10.1021/acs.biomac.0c00620. URL `https://doi.org/10.1021/acs.biomac.0c00620`. PMID: 32539358.

[7] Celine E. Eidhammer. Block polysaccharides: Pdha activated ha blocks and biotin activated β-1,3-glucan.

[8] Odin W. Haarnerg. *Towards Dextran-Based Block Polysaccharides*. NTNU, 2018. Master's thesis.

[9] K Van de Velde and P Kiekens. Biopolymers: overview of several properties and consequences on their applications. *Polymer Testing*, 21(4):433–442, 2002. ISSN 0142-9418. doi: https://doi.org/10.1016/S0142-9418(01)00107-6. URL https://www.sciencedirect.com/science/article/pii/S0142941801001076.

[10] Amalie Solberg, Ingrid V. Mo, Line Aa. Omtvedt, Berit L. Strand, Finn L. Aachmann, Christophe Schatz, and Bjørn E. Christensen. Carbohydr polym special issue invited contribution: Click chemistry for block polysaccharides with dihydrazide and dioxyamine linkers - a review. *Carbohydrate Polymers*, page 118840, 2021. ISSN 0144-8617. doi: https://doi.org/10.1016/j.carbpol.2021.118840. URL https://www.sciencedirect.com/science/article/pii/S0144861721012273.

[11] Hilde Kristoffersen. *β-1,3-glucan and β-1,3-glucan-based diblock polysaccharides: Preparation, characterization, and solution behavior*. NTNU, 2021. Master's thesis.

[12] Christophe Schatz and Sébastien Lecommandoux. Polysaccharide-containing block copolymers: Synthesis, properties and applications of an emerging family of glycoconjugates. *Macromolecular Rapid Communications*, 31(19):1664–1684, 2010. doi: https://doi.org/10.1002/marc.201000267. URL https://onlinelibrary.wiley.com/doi/abs/10.1002/marc.201000267.

[13] Godfrey Chi-Fung Chan, Wing Keung Chan, and Daniel Man-Yuen Sze. The effects of -glucan on human immune and cancer cells. *Journal of Hematology & Oncology*, 2(1):25, 2009. doi: 10.1186/1756-8722-2-25. URL https://doi.org/10.1186/1756-8722-2-25.

[14] Wenshui Xia, Ping Liu, Jiali Zhang, and Jie Chen. Biological activities of chitosan and chitooligosaccharides. *Food Hydrocolloids*, 25(2):170–179, 2011. ISSN 0268-005X. doi: https://doi.org/10.1016/j.foodhyd.2010.

03.003. URL https://www.sciencedirect.com/science/article/pii/S0268005X10000469. Dietary Fibre and Bioactive Polysaccharides.

[15] K. Jung, Y. Ha, S.-K. Ha, D. U. Han, D.-W. Kim, W. K. Moon, and C. Chae. Antiviral effect of saccharomyces cerevisiae-glucan to swine influenza virus by increased production of interferon- and nitric oxide. *Journal of Veterinary Medicine, Series B*, 51(2):72–76, 2004. doi: https://doi.org/10.1111/j.1439-0450.2004.00732.x. URL https://onlinelibrary.wiley.com/doi/abs/10.1111/j.1439-0450.2004.00732.x.

[16] Gordon D. Brown, Jurgen Herre, David L. Williams, Janet A. Willment, Andrew S. J. Marshall, and Siamon Gordon. Dectin-1 Mediates the Biological Effects of -Glucans . *Journal of Experimental Medicine*, 197(9):1119–1124, 04 2003. ISSN 0022-1007. doi: 10.1084/jem.20021890. URL https://doi.org/10.1084/jem.20021890.

[17] Fen Qin. Chemical and physical characterization of bioactive soluble [1→ 3]-ßd-glucans [sbg] from saccharomyces sp. 2012.

[18] Soliman OY, Alameh MG, De Cresenzo G, Buschmann MD, and Lavertu M. Efficiency of chitosan/hyaluronan-based mrna delivery systems in vitro: Influence of composition and structure. 109(4):1581–1593, 2020. doi: 10.1016/j.xphs.2019.12.020. URL https://doi.org/10.1016/j.xphs.2019.12.020.

[19] Hongbo Feng, Xinyi Lu, Weiyu Wang, Nam-Goo Kang, and Jimmy W. Mays. Block copolymers: Synthesis, self-assembly, and applications. *Polymers*, 9(10), 2017. ISSN 2073-4360. URL https://www.mdpi.com/2073-4360/9/10/494.

[20] Anastasia S. Volokhova, Kevin J. Edgar, and John B. Matson. Polysaccharide-containing block copolymers: synthesis and applications. *Mater. Chem. Front.*, 4:99–112, 2020. doi: 10.1039/C9QM00481E. URL http://dx.doi.org/10.1039/C9QM00481E.

[21] Benjamin B. Breitenbach, Ira Schmid, and Peter R. Wich. Amphiphilic polysaccharide block copolymers for ph-responsive micellar nanoparticles.

Biomacromolecules, 18(9):2839–2848, 2017. doi: 10.1021/acs.biomac.7b00771. URL https://doi.org/10.1021/acs.biomac.7b00771. PMID: 28745492.

[22] Xiao-Hua Hu and Shisheng Xiong. Fabrication of nanodevices through block copolymer self-assembly. *Frontiers in Nanotechnology*, 4, 2022. ISSN 2673-3013. doi: 10.3389/fnano.2022.762996. URL https://www.frontiersin.org/article/10.3389/fnano.2022.762996.

[23] Nan Zhang, Patricia R. Wardwell, and Rebecca A. Bader. Polysaccharide-based micelles for drug delivery. *Pharmaceutics*, 5(2):329–352, 2013. ISSN 1999-4923. doi: 10.3390/pharmaceutics5020329. URL https://www.mdpi.com/1999-4923/5/2/329.

[24] Bjørn E. Christensen. *Compendium TBT4135 Biopolymers*. NTNU, Department of Biotechnology and Food Science, 2020.

[25] Michael J. Gidley and Katsuyoshi Nishinari. Chapter 2.2 - physico-chemistry of (1,3)--glucans. In Antony Bacic, Geoffrey B. Fincher, and Bruce A. Stone, editors, *Chemistry, Biochemistry, and Biology of 1-3 Beta Glucans and Related Polysaccharides*, pages 47–118. Academic Press, San Diego, 2009. ISBN 978-0-12-373971-1. doi: https://doi.org/10.1016/B978-0-12-373971-1.00003-0. URL https://www.sciencedirect.com/science/article/pii/B9780123739711000030.

[26] T. H. Nguyen, G. H. Fleet, and P. L. Rogers. Composition of the cell walls of several yeast species. *Applied Microbiology and Biotechnology*, 50(2):206–212, 1998. doi: 10.1007/s002530051278. URL https://doi.org/10.1007/s002530051278.

[27] Antje Müller, Harry Ensley, Henry Pretus, Rose McNamee, Ernest Jones, Emily McLaughlin, Wilma Chandley, William Browder, Douglas Lowman, and David Williams. The application of various protic acids in the extraction of (1 → 3)--d-glucan from saccharomyces cerevisiae. *Carbohydrate Research*, 299(3):203–208, 1997. ISSN 0008-6215. doi: https://doi.org/10.1016/S0008-6215(97)

00004-9. URL https://www.sciencedirect.com/science/article/pii/S0008621597000049.

[28] David L. Williams, Rose B. McNamee, Ernest L. Jones, Henry A. Pretus, Harry E. Ensley, I.William Browder, and Nicholas R. Di Luzio. A method for the solubilization of a (1→3)--d-glucan isolated from saccharomyces cerevisiae. *Carbohydrate Research*, 219:203–213, 1991. ISSN 0008-6215. doi: https://doi.org/10.1016/0008-6215(91)89052-H. URL https://www.sciencedirect.com/science/article/pii/000862159189052H.

[29] Rolf E. Engstad and Brre Robertsen. Recognition of yeast cell wall glucan by atlantic salmon (salmo salar l.) macrophages. *Developmental Comparative Immunology*, 17(4):319–330, 1993. ISSN 0145-305X. doi: https://doi.org/10.1016/0145-305X(93)90004-A. URL https://www.sciencedirect.com/science/article/pii/0145305X9390004A.

[30] Shaoping Nie, Steve W. Cui, and Mingyong Xie. Chapter 3 - beta-glucans and their derivatives. In Shaoping Nie, Steve W. Cui, and Mingyong Xie, editors, *Bioactive Polysaccharides*, pages 99–141. Academic Press, 2018. ISBN 978-0-12-809418-1. doi: https://doi.org/10.1016/B978-0-12-809418-1.00003-4. URL https://www.sciencedirect.com/science/article/pii/B9780128094181000034.

[31] Yan Meng, Fengzhi Lyu, Xiaojuan Xu, and Lina Zhang. Recent advances in chain conformation and bioactivities of triple-helix polysaccharides. *Biomacromolecules*, 21(5):1653–1677, 2020. doi: 10.1021/acs.biomac.9b01644. URL https://doi.org/10.1021/acs.biomac.9b01644. PMID: 31986015.

[32] J. S. D. Bacon, V C Farmer, D. Jones, and Irene F. Taylor. The glucan components of the cell wall of baker's yeast (Saccharomyces cerevisiae) considered in relation to its ultrastructure. *Biochemical Journal*, 114(3):557–567, 09 1969. ISSN 0006-2936. doi: 10.1042/bj1140557. URL https://doi.org/10.1042/bj1140557.

[33] Susan M Tosh, Peter J Wood, Qi Wang, and John Weisz. Structural character-

istics and rheological properties of partially hydrolyzed oat -glucan: the effects of molecular weight and hydrolysis method. *Carbohydrate Polymers*, 55 (4):425–436, 2004. ISSN 0144-8617. doi: https://doi.org/10.1016/j.carbpol.2003.11.004. URL https://www.sciencedirect.com/science/article/pii/S0144861703003151.

[34] Lee SH, Jang GY, Hwang IG, Kim HY, Woo KS, Kim KJ, Lee MJ, Kim TJ, Lee J, and Jeong HS. Physicochemical properties of -glucan from acid hydrolyzed barley. *Prev Nutr Food Sci*, 20(2):110–118, 2015. doi: 10.3746/pnf.2015.20.2.110. URL https://doi.org/10.3746/pnf.2015.20.2.110.

[35] Pelizon AC, Kaneno R, Soares AM, Meira DA, and Sartori A. Immunomodulatory activities associated with beta-glucan derived from saccharomyces cerevisiae. 2005.

[36] Di Luzio NR and Williams DL. Protective effect of glucan against systemic staphylococcus aureus septicemia in normal and leukemic mice. 1978.

[37] J. K. Czop. The role of -glucan receptors on blood and tissue leukocytes in phagocytosis and metabolic activation. *Pathology and Immunopathology Research*, 5(3-5):286–296, 1986. doi: 10.1159/000157022. URL https://www.karger.com/DOI/10.1159/000157022.

[38] B. ROBERTSEN, G. RRSTAD, R. ENGSTAD, and J. RAA. Enhancement of non-specific disease resistance in atlantic salmon, salmo salar l., by a glucan from saccharomyces cerevisiae cell walls. *Journal of Fish Diseases*, 13(5):391–400, 1990. doi: https://doi.org/10.1111/j.1365-2761.1990.tb00798.x. URL https://onlinelibrary.wiley.com/doi/abs/10.1111/j.1365-2761.1990.tb00798.x.

[39] S. Islam, M. A. Rahman Bhuiyan, and M. N. Islam. Chitin and chitosan: Structure, properties and applications in biomedical engineering. *Journal of Polymers and the Environment*, 25(3):854–866, 2017. doi: 10.1007/s10924-016-0865-5. URL https://doi.org/10.1007/s10924-016-0865-5.

[40] Kristoffer Tømmeraas, Kjell M Vårum, Bjørn E Christensen, and Olav Smid-

srød. Preparation and characterisation of oligosaccharides produced by nitrous acid depolymerisation of chitosans. *Carbohydrate Research*, 333(2):137–144, 2001. ISSN 0008-6215. doi: https://doi.org/10.1016/S0008-6215(01)00130-6. URL https://www.sciencedirect.com/science/article/pii/S0008621501001306.

[41] Janos Zempleni, Subhashinee S.K. Wijeratne, and Yousef I. Hassan. Biotin. *BioFactors*, 35(1):36–46, 2009.

[42] A. Marquet. Biotin biosynthesis. *Pure and Applied Chemistry*, 65(6):1249–1252, 1993. doi: doi:10.1351/pac199365061249. URL https://doi.org/10.1351/pac199365061249.

[43] Liang Tong. Structure and function of biotin-dependent carboxylases. *Cellular and Molecular Life Sciences*, 70(5):863–891, 2013. doi: 10.1007/s00018-012-1096-0. URL https://doi.org/10.1007/s00018-012-1096-0.

[44] Grover L. Waldrop, Ivan Rayment, and Hazel M. Holden. Three-dimensional structure of the biotin carboxylase subunit of acetyl-coa carboxylase*. *Biochemistry*, 33(34):10249–10256, 1994. doi: 10.1021/bi00200a004. URL https://pubs.acs.org/doi/pdf/10.1021/bi00200a004.

[45] J L Guesdon, T Ternynck, and S Avrameas. The use of avidin-biotin interaction in immunoenzymatic techniques. *Journal of Histochemistry & Cytochemistry*, 27(8):1131–1139, 1979. doi: 10.1177/27.8.90074. URL https://doi.org/10.1177/27.8.90074. PMID: 90074.

[46] Meir Wilchek and Edward A Bayer. The avidin-biotin complex in immunology. *Immunology Today*, 5(2):39–43, 1984. ISSN 0167-5699. doi: https://doi.org/10.1016/0167-5699(84)90027-6. URL https://www.sciencedirect.com/science/article/pii/0167569984900276.

[47] Katrin Knop, Richard Hoogenboom, Dagmar Fischer, and UlrichS. Schubert. Poly(ethylene glycol) in drug delivery: Pros and cons as well as potential alternatives. *Angewandte Chemie International Edition*, 49(36):6288–

6308, 2010. doi: https://doi.org/10.1002/anie.200902672. URL https://onlinelibrary.wiley.com/doi/abs/10.1002/anie.200902672.

[48] John W. Nicholson. *The Chemistry of Polymers*. RSC Publishing, 2006. ISBN 0-85404-684-4. 3rd edition.

[49] Ahmed F. Abdel-Magid, Kenneth G. Carson, Bruce D. Harris, Cynthia A. Maryanoff, and Rekha D. Shah. Reductive amination of aldehydes and ketones with sodium triacetoxyborohydride. studies on direct and indirect reductive amination procedures1. *The Journal of Organic Chemistry*, 61(11):3849–3862, 1996. doi: 10.1021/jo960057x. URL https://doi.org/10.1021/jo960057x. PMID: 11667239.

[50] M.Ø. Dalheim. Chemically modified alginates and chitosans. lateral and terminal functionalization by reductive amination. 2016.

[51] Zicai Sun, Zheng Wei, and Kemei Wei. A model for predicting the optimal conditions for labeling the carbohydrates with the amine derivatives by reductive amination (supplementry material). *Letters in Organic Chemistry*, 6(7):549–551, 2009. ISSN 1570-1786/1875-6255. doi: 10.2174/157017809789869447. URL http://www.eurekaselect.com/article/30267.

[52] Vanina A. Cosenza, Diego A. Navarro, and Carlos A. Stortz. Usage of -picoline borane for the reductive amination of carbohydrates. *ARKIVOC*, (7):182–194, 2011. doi: 10.3998/ark.5550190.0012.716. URL http://dx.doi.org/10.3998/ark.5550190.0012.716.

[53] Shinya Sato, Takeshi Sakamoto, Etsuko Miyazawa, and Yasuo Kikugawa. One-pot reductive amination of aldehydes and ketones with -picoline-borane in methanol, in water, and in neat conditions. *Tetrahedron*, 60(36):7899–7906, 2004. ISSN 0040-4020. doi: https://doi.org/10.1016/j.tet.2004.06.045. URL https://www.sciencedirect.com/science/article/pii/S0040402004009135.

[54] Ozlem Coskun. Separation techniques: Chromatography. 3(2):156–160, Nov

2016. doi: 10.14744/nci.2016.32757. URL https://www.ncbi.nlm.nih.gov/pmc/articles/PMC5206469/.

[55] E. Lundanes, L. Reubsaet, and T. Greibrokk. *Chromatography – Basic Principles, Sample Preparations and Related Methods*. Weinheim, Germany: Wiley-VCH Verlag GmbH Co. KGaA, 2013. ISBN 978-3-527-33620-3.

[56] R. W. A. Oliver. *HPLC of Macromolecules; a practical approach*. Oxford University Press Inc., 1998. ISBN 0199635714. 2nd edition, Ch. 4 7.

[57] Sadao Mori and Howard G. Barth. *Size Exclusion Chromatography*, chapter 1, 2. Springer-Verlag, New York, 1999.

[58] Robert M. Siverstein, Francis X. Webster, David J. Kiemle, and David L. Bryce. *Spectrometric Identification of Organic Compounds*. Wiley, 2015. ISBN 978-0-470-61637-6. 8th edition, Ch. 3.

[59] Hiroshi Nabetani, Mitsutoshi Nakajima, Atsuo Watanabe, Shin ichi Nakao, and Shoji Kimura. Effects of osmotic pressure and adsorption on ultrafiltration of ovalbumin. *AIChE Journal*, 36(6):907–915, 1990.

[60] Stefan Freimund, Martin Sauter, Othmar Käppeli, and Hans Dutler. A new non-degrading isolation process for 1,3--d-glucan of high purity from baker's yeast saccharomyces cerevisiae. *Carbohydrate Polymers*, 54(2):159–171, 2003. ISSN 0144-8617. doi: https://doi.org/10.1016/S0144-8617(03)00162-0. URL https://www.sciencedirect.com/science/article/pii/S0144861703001620.

[61] Hiroyuki Kono, Nobuhiro Kondo, Katsuki Hirabayashi, Makoto Ogata, Kazuhide Totani, Shinya Ikematsu, and Mitsumasa Osada. Two-dimensional nmr data of a water-soluble -(1→3, 1→6)-glucan from aureobasidium pullulans and schizophyllan from schizophyllum commune. *Data in Brief*, 15:382–388, 2017. ISSN 2352-3409. doi: https://doi.org/10.1016/j.dib.2017.09.067. URL https://www.sciencedirect.com/science/article/pii/S2352340917305073.

[62] G. Gelardi and R.J. Flatt. 11 - working mechanisms of water reducers and superplasticizers. In Pierre-Claude Aïtcin and Robert J Flatt, editors, *Science and Technology of Concrete Admixtures*, pages 257–278. Woodhead Publishing, 2016. ISBN 978-0-08-100693-1. doi: https://doi.org/10.1016/B978-0-08-100693-1.00011-4. URL https://www.sciencedirect.com/science/article/pii/B9780081006931000114.

[63] Alain Domard, Claude Gey, and François Taravel. Glucosamine oligomers: 2. n.m.r. studies on a dp3. *International Journal of Biological Macromolecules*, 13(2):105–109, 1991. ISSN 0141-8130. doi: https://doi.org/10.1016/0141-8130(91)90057-2. URL https://www.sciencedirect.com/science/article/pii/0141813091900572.

A Appendix: Chemical data

Relevant chemical data used in calculations are given in table A1.

Table A1: Chemical data. [a]Calculated based on an average of DP 17.

Substance	Molecular weight [Da]
H_2O	18
NaCl	58.44
Na_2SO_4	142.04
HAc	60.05
NaAc	82.03
D-glucose	162
D-glucosamine	161
2,5-Anhydro-D-mannose	162.14
PDHA	179.05
PB	106.96
SBG_4	666
SBG_8	1314
SBG_{14}	2286
$SBG_{(15-19)}$	2772[a]
SBG_{10}-PDHA	1817
$D_{11}M$	1949
Biotin-$dPEG_3$ oxyamine	471.01

B Appendix: ^{1}H-NMR analysis of SBG

A non-purified sample of hydrolysed SBG (221-7) was characterized using ^{1}H-NMR, displayed in figure B.1. The average DP was calculated to be 7, using Equation 2.

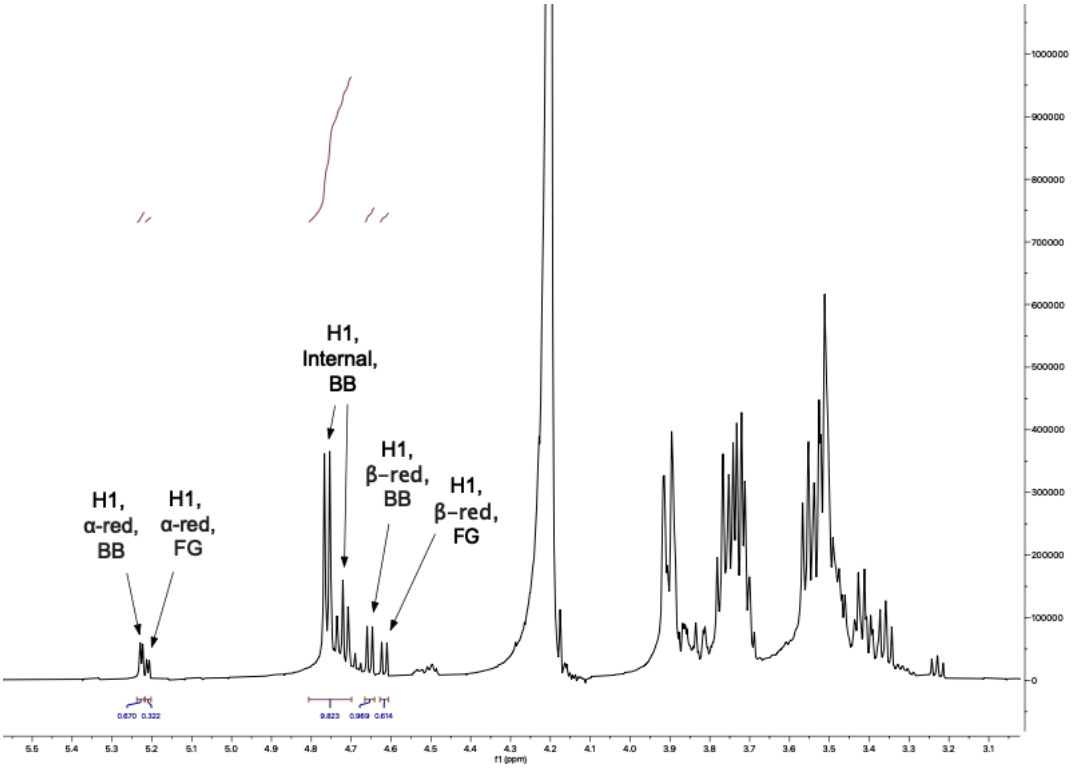

Figure B.1: ^{1}H-NMR spectra of non-purified, SBG (221-7) hydrolysate (5mg/ml, 0.1M Na_2SO_4, 99°C, 75 min) at 82°C. Average DP = 7. 600 MHz.

C Appendix: Desalting of hydrolysed SBG

Standard curve used in estimating salt concentration

The standard curve of Na_2SO_4 used in determination of salt concentration based on measured conductivity, if given in Figrure C.2.

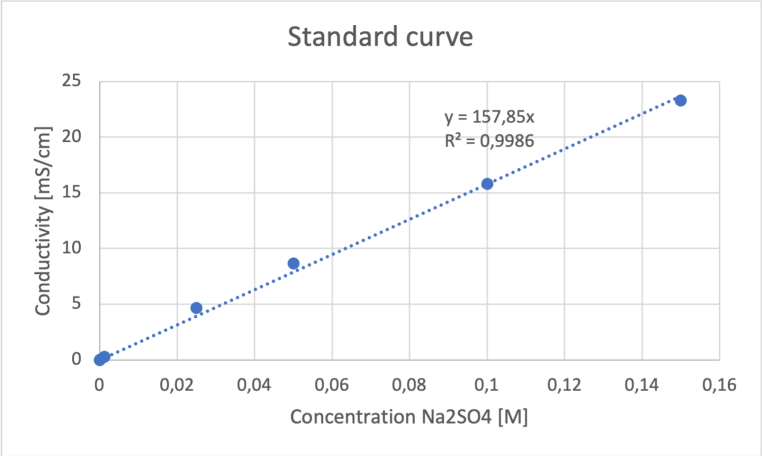

Figure C.2: The standard curve of Na_2SO_4 with conductivity plotted against concentration

Centricon filtration

Photo C.3 shows the accumulation of substance on the centrigual Centricon filters.

Figure C.3: Photo of the centrifugal Centricon filters with accumulated SBG oligomers

D Appendix: SBG=PDHA

In order to evaluate if a high concentration of salt effects the conjugation rate to a significant level, an conjugation of non-purified SBG hydrolysate was conducted and compared to a dialysed and thus purified SBG hydrolysate. This comparison is of interest due to the time-consuming process of dialysis as well as often resulting in significant loss of polymers with DP < ~ 6.

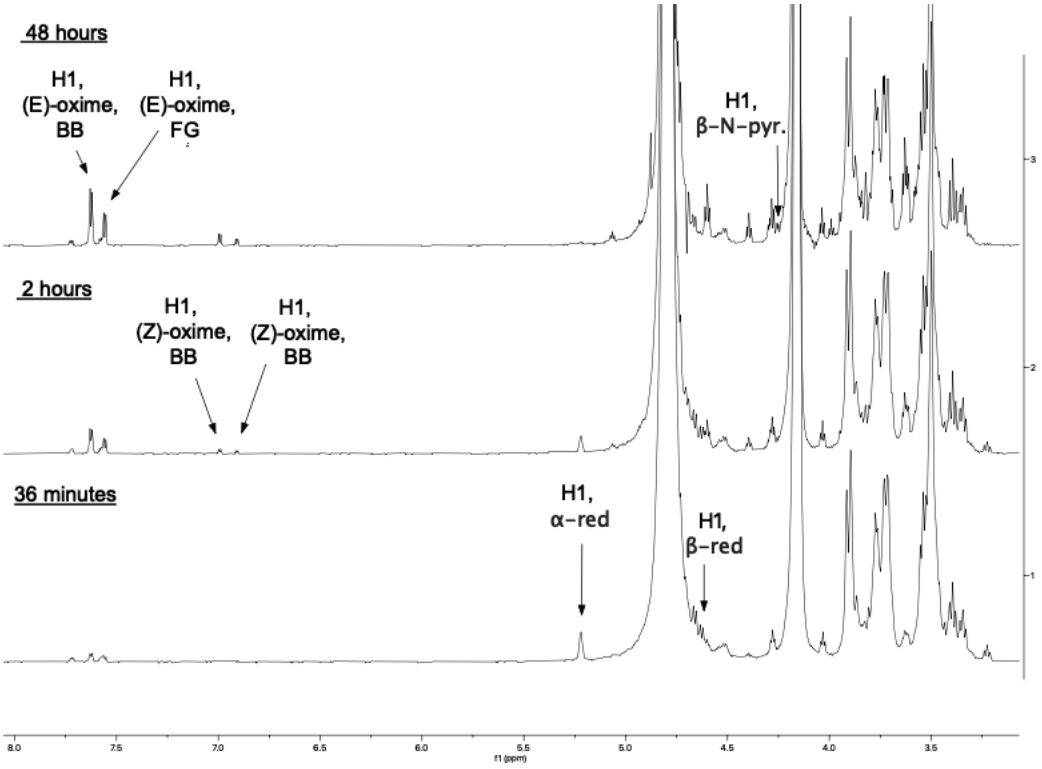

Figure D.4: Conjugation of non-purified SBG hydrolysate with PDHA (~ 10 eq. PDHA, pH 4, RT). BB: Backbone. FG: Free glucose [8].

Kinetics study from PDHA activation of SBG, from dialysed hydrolysate in figure D.5a and non-purified Hydrolysate in figure D.5b. Model used in kinetics study was provided by Professor Bjørn E. Christensen at Department of Biotechnology and Food Science, NTNU.

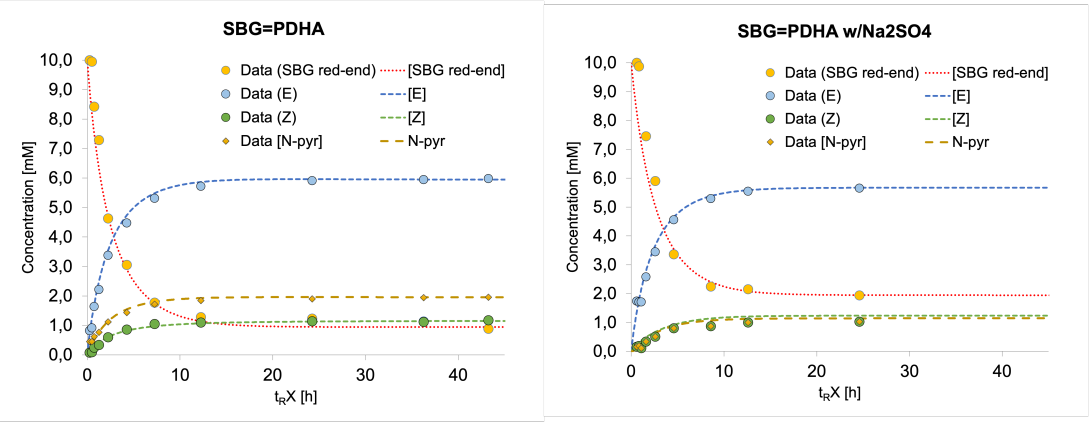

(a) **(b)**

Figure D.5: a) Kinetics study of PDHA activation of hydrolysed and dialysed SBG (10x eq. PDHA, pH 4, RT). **b)** Kinetics study of SBG hydrolysate (~ 10x eq. PDHA, pH 4, RT)

E Appendix: Characterisation of in-house chitosan

An ^{1}H-NMR analysis was conducted on in-house $D_{11}M$ prepared by J.E. Pedersen in 2020, shown in Figure E.6. It was conducted to validate the stability of the oligomer and fraction of oligomers with M-units as reducing ends. This information was necessary to achieve right ratio between M-units and SBG-PDHA during conjugation. Peak assignment was determined from Ingrid *et al.* [3] and Domard *et al.* [63].

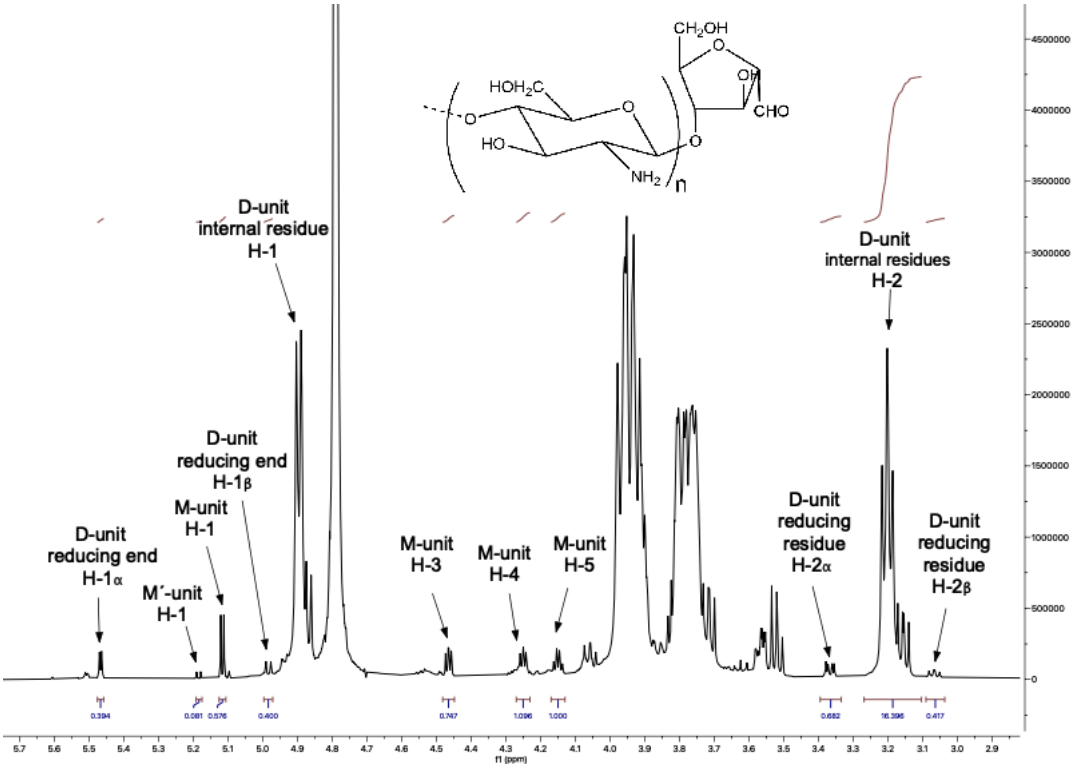

Figure E.6: ^{1}H-NMR spectra of in-house $D_{11}M$, prepared by J.E. Pedersen in 2020.

F Appendix: NMR Biotin-PEG$_3$ oxyamine

^{1}H-NMR spectra of Biotin-PEG$_3$ used in calculation of imine reduction of SBG$_n$=PEG$_3$-biotin. A peak on biotin was set as standard (= 1.0) in the NMR spectra of both Biotin-PEG$_3$ and SBG$_n$=PEG$_3$-biotin spectra. The integral of the the secondary amine in PEG$_3$-biotin linkage could then be compared to the reduced SBG$_n$=PEG$_3$-biotin diblock, and the integral of secondary amine in SBG$_n$-PEG$_3$ linkage. In a 100% reduction, the area of secondary amines in PEG$_3$-biotin linkage and SBG$_n$-PEG$_3$ linkage would be equal, as both corresponds to two hydrogens.

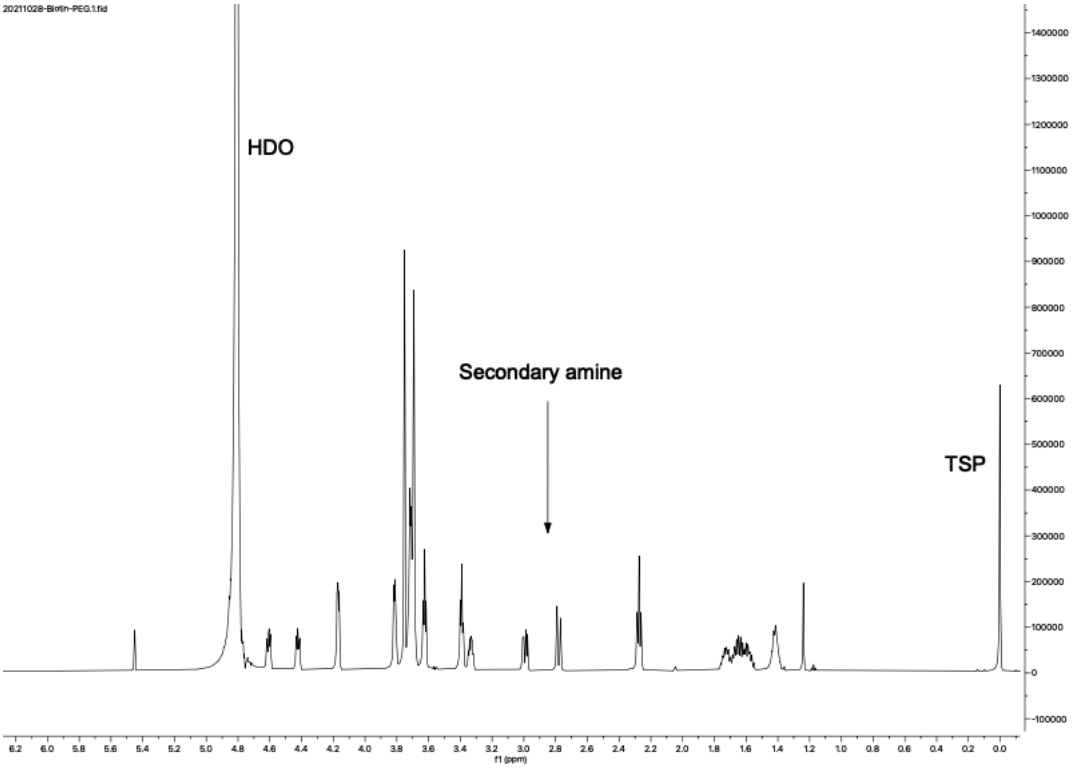

Figure F.7: ^{1}-NMR analysis of pure biotin-PEG$_3$ oxyamine. Collected from related specialisation project [7].

G Appendix: SBG_m-PEG_3-Biotin

SBG_m=PEG_3-Biotin conjugation

The time course NMR-analysis of SBG_{14}-PEG_3-biotin and SBG_{15-19}-PEG_3-biotin, using protocol described in Section 3.9.1.

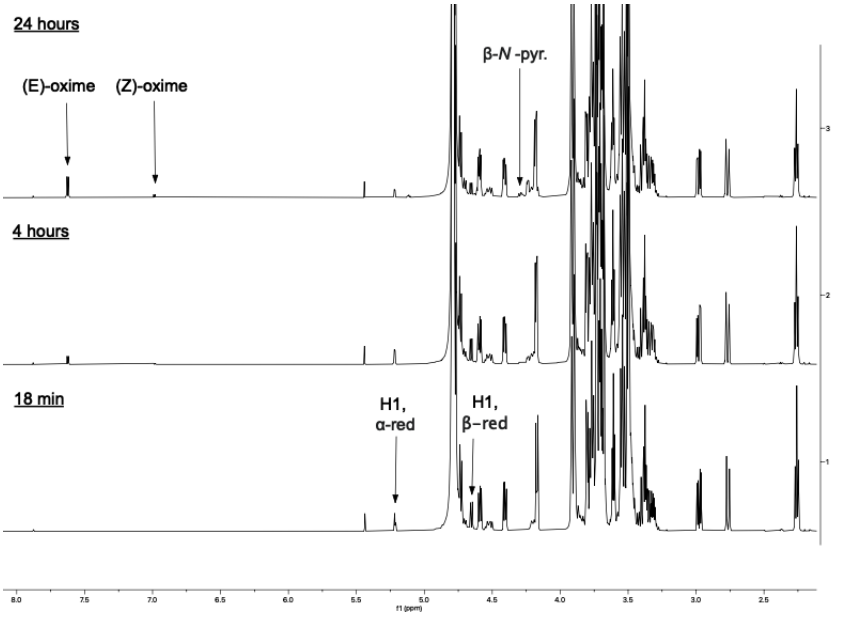

(a)

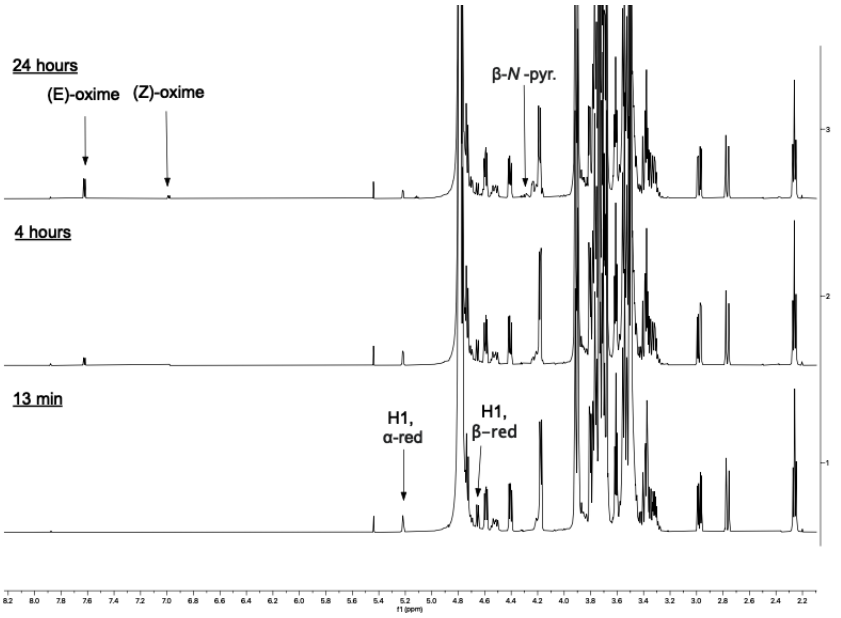

(b)

Figure G.8: The time-course analysis from conjugation of **a)** SBG_{14}-PEG_3-biotin and **b)** SBG_{15-19}-PEG_3-biotin

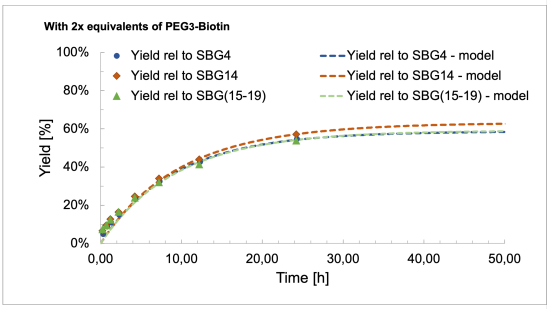

(a) Yield model for all three samples

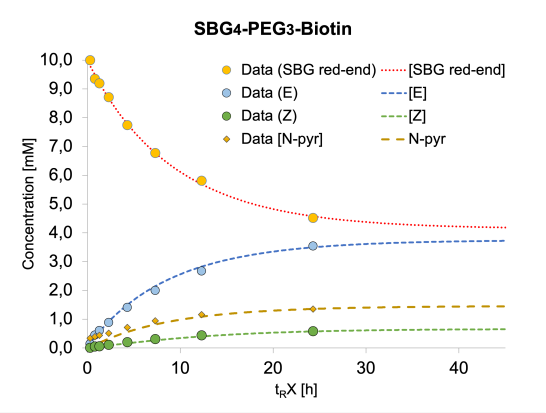

(b) Kinetics study SBG4

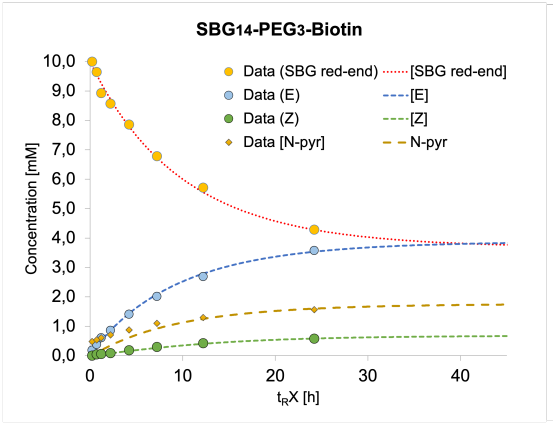

(c) Kinetics study SBG14

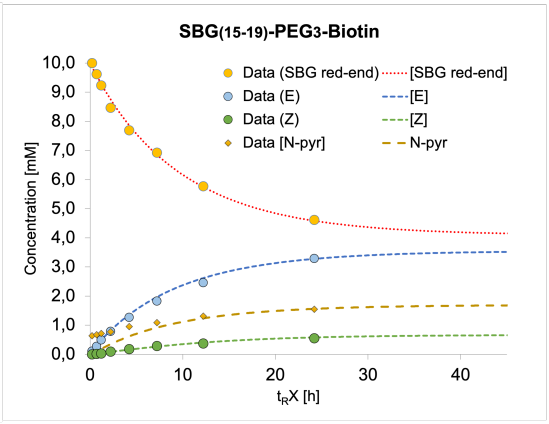

(d) Kinetics study SBG15-19

Figure G.9: Kinetics data from reductive amination of SBG_m=PEG_3-biotin.

SBG_m-EPG_3-Biotin; imine reduction

The reduction yield of SBG_4-PEG_3-Biotin, SBG_{14}-PEG_3-Biotin and SBG_{15-19}-PEG_3-Biotin was calculated based on the integral of (E)-oxime prior to reduction, compared to the integral after reduction and purification. A hydrogen from biotin (peak 2.3 ppm) was set as standard for comparison. The area at reduction, i.e. when PB was added to solution (41h for DP4 and 45h for DP14 and DP15-19), was calculated using equation G.1. The yield at 41h was determined based on the kinetics analysis of the conjugation, Table 3. Following, equation G.2 was used to calculated to yield of reduction.

$$A_{41h} = (\frac{A_{(E)-oximes,24h}}{Yield_{24h}}) \cdot Yield_{41h} \tag{G.1}$$

$$Yield_{Reduction} = \frac{A_{41h} - A_{Reduced}}{A_{41h}} \tag{G.2}$$

Reduction:

SBG4-PEG3-Biotin

Yield 24h: 0,538 Based on kinetics model
Yield 41h: 0,578

Area (E)-oxime, 41h (calculated):	Area after reduction	Yield	**Yield [%]**
0,119	0,045	0,62	**62**

SBG14-PEG3-Biotin

Yield 24h: 0,571 Based on kinetics model
Yield 45h: 0,623

Area (E)-oxime, 45h (calculated):	Area after reduction	Yield	**Yield [%]**
0,115	0,034	0,70	**70**

SBG15-19-PEG3-Biotin

Yield 24h: 0,541 Based on kinetics model
Yield 45h: 0,585

Area (E)-oxime, 45h (calculated):	Area after reduction	Yield	**Yield [%]**
0,107	0,018	0,83	**83**

Mass of SBG_m-PEG_3-Biotin

The measured conductivity and calculated mass of SBG_m-PEG_3-biotin is presented in Table A2.

	Prior to dialysis	After dialysis				
Diblock	Mass NaCl [mg]	Conductivity [mS/cm]	Mass NaCl [mg]	Weighted product [mg]	Estimated mass diblocks [mg]	Theoretical mass diblocks [mg]
SBG_4-PEG_3-Biotin	~ 240	5.6	4.9	14.2	9.3	0.2
SBG_{14}-PEG_3-Biotin	~ 410	13.0	11.4	39.2	27.8	4.1
SBG_{15-19}-PEG_3-Biotin	~ 720	20.5	17.9	61.9	44.0	5.6

Table A2: Mass of SBG_4-PEG_3-Biotin, SBG_{14}-PEG_3-Biotin and SBG_{15-19}-PEG_3-Biotin after conjugation (10mM, 1:2 [Equi.], pH 4, RT, 41/45h)), reduction (20x PB, 40 °C, 124h) and purification (3.5 kDa dialysis, 2 shifts). Theoretical mass is calculated through comparing the area and known mass of biotin-PEG_3 with area of diblocks. Mass prior to dialysis is calculated based on total volume of the SEC-fractions and NaCl concentration in buffer (0.1M).

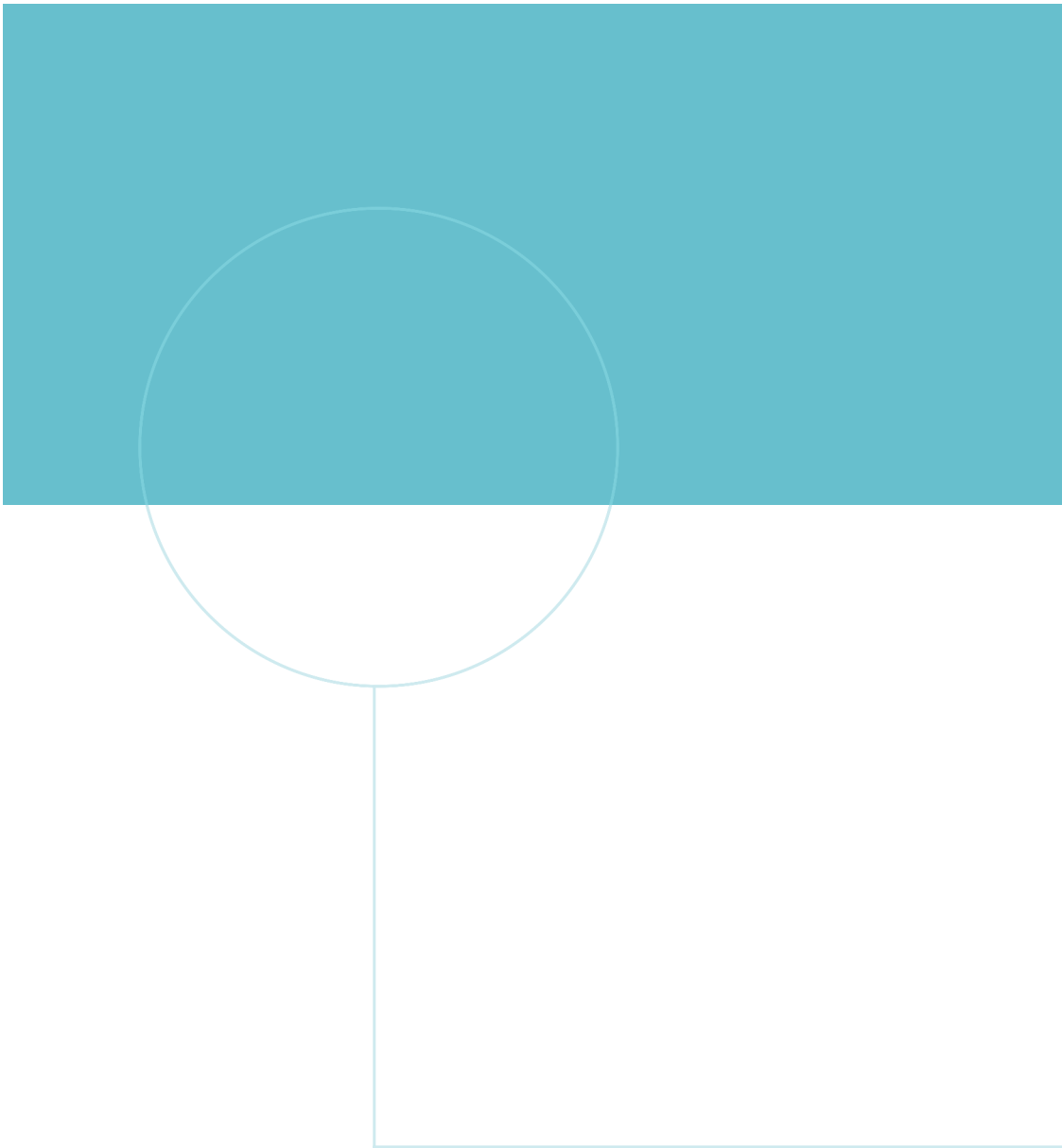

NTNU

Norwegian University of
Science and Technology